A Role for sFRP5 in Adipocyte Biology and Obesity

by

Tyler C. Prestwich

A dissertation submitted in partial fulfillment
of the requirements for the degree of
Doctor of Philosophy
(Cellular and Molecular Biology)
in The University of Michigan
2008

Doctoral Committee:

Professor Ormond A. MacDougald, Chair
Professor Charles Burant
Professor Eric R. Fearon
Associate Professor Kenneth M. Cadigan
Assistant Professor Peter C. Lucas

Table of Contents

List of Figures

Chapter I

Wnt/β-catenin Signaling in Adipogenesis and Metabolism

Summary

Adipocyte differentiation consists of a complex series of events in which scores of cellular and extracellular factors interact to transform a fibroblast-like preadipocyte into a mature, lipid-filled adipocyte. Many of the pathways influencing this process have been identified using well-characterized preadipocyte culture systems and have subsequently been confirmed in animal models. Research conducted over the last decade has established the Wnt/β-catenin signaling pathway as an important regulator of adipocyte differentiation. While initial reports implicated activators of Wnt/β-catenin signaling as potent inhibitors of adipogenesis, recent investigations of mesenchymal cell fate, obesity, and type 2 diabetes highlight significant additional roles for Wnt signaling in metabolism and adipocyte biology.

Introduction

Adipogenesis is the process by which mesenchymal precursor cells differentiate into adipocytes, which store lipid and serve as central regulators of metabolism [1-3]. Identifying key factors that control adipocyte differentiation and metabolism is vital to understanding adipose tissue biology and pathology. The

transcriptional cascade controlling adipogenesis has been well characterized over the past two decades and mechanisms by which master adipocyte regulators act are now beginning to be fully elucidated. Peroxisome proliferator-activated receptor γ (PPARγ) and CCAAT/enhancer binding protein α (C/EBPα) are the chief regulators thought to coordinately direct the adipogenic program. PPARγ is both necessary and sufficient for preadipocyte differentiation [1], while C/EBPα appears to be important for the acquisition of insulin sensitivity in adipocytes [4]. The current state of research on these important transcriptional regulators has been recently reviewed elsewhere [2,3].

Transcription factors that control the cascade of events leading to a fully differentiated adipocyte act downstream of complex signaling pathways that integrate signals from the surrounding microenvironment. Over the past several years, the field of adipogenesis has seen an upsurge in the number of reports implicating locally secreted or circulating extracellular factors as regulators of preadipocyte differentiation [3]. One of the extracellular signaling pathways now known to affect adipogenesis is the Wnt pathway. Wnts are an evolutionarily conserved family of secreted lipidated glycoproteins with well-established roles in cellular proliferation, differentiation, and polarity during embryogenesis [5,6]. More recently, Wnt signaling has been shown to modulate additional developmental and physiological processes, including aspects of adipocyte biology [7-11]. In this review, we provide an overview of the research revealing a principal role for Wnt signaling in adipogenesis. We present a brief chronology of the studies demonstrating Wnt inhibition of adipocyte differentiation *in vitro* and *in*

vivo, culminating with the recent linkages of Wnt pathway members to human diseases including obesity and type 2 diabetes. Finally, we examine the latest reports providing mechanistic insight into how Wnt signaling functions to block adipogenesis and regulate mesenchymal cell fate.

Wnt Signaling Regulates Adipogenesis *In Vitro* and *In Vivo*:

Wnts are secreted proteins that act though autocrine and paracrine mechanisms to influence the development of many cell types [5,6]. Although Wnts can inhibit preadipocyte differentiation through both β-catenin-dependent and -independent mechanisms [12], current genetic evidence supports β-catenin as a particularly crucial regulator of adipogenesis [13]. In the canonical Wnt signaling pathway, β-catenin plays a central role as a transcriptional coactivator. Upon binding of Wnt ligands to frizzled receptors and low density lipoprotein receptor-related protein (LRP) coreceptors, cytoplasmic β-catenin is hypophosphorylated, stabilized, and translocated into the nucleus where it binds to and coactivates members of the T-cell factor/lymphoid-enhancing factor (TCF/LEF) family of transcription factors to direct target gene expression (Fig. 1.1).

In Vitro

Studies utilizing preadipocyte lines originally demonstrated that ectopic expression of Wnt1, an activator of Wnt/β-catenin signaling, potently represses adipogenesis (Fig. 1.1) [7,11]. Similarly, pharmacological agents that activate

canonical Wnt signaling and stabilize free cytosolic β-catenin also block preadipocyte differentiation [7,8]. Conversely, inhibition of Wnt signaling in preadipocytes stimulates differentiation [7,8,14-16], suggesting that preadipocytes produce endogenous Wnts that strongly repress adipogenesis. One endogenous factor is Wnt10b, expression of which is high in dividing and confluent preadipocytes and is rapidly downregulated in response to elevated cAMP during induction of differentiation [7,8]. Furthermore, constitutive expression of *Wnt10b* stabilizes free cytosolic β-catenin and inhibits adipogenesis (Fig. 1.1) [7]. While considerable evidence suggests that Wnt10b is a prominent extracellular regulator of adipogenesis, other Wnt ligands are also expressed and likely contribute to the process. For example, Wnt6 and Wnt10a have been identified as endogenous regulators of brown adipocyte development [17,18]. Additionally, Wnt5b is transiently induced during adipogenesis and acts through an unknown mechanism to destabilize β-catenin and promote differentiation [19,20]**,** indicating that preadipocytes integrate inputs from a variety of competing Wnt signals (Fig. 1.1). One of the mechanisms by which Wnt/β-catenin signaling inhibits adipogenesis is thought to involve dysregulated expression of cyclin dependent kinase inhibitors, p21 and p27 [21].

Adipogenesis is regulated not only by expression of specific Wnt ligands, but also by expression of factors that inhibit the Wnt/β-catenin pathway. For example, Li *et al.* recently reported that a nuclear β-catenin antagonist, chibby (Cby), is expressed in adipose tissue and is induced during differentiation of 3T3-L1 preadipocytes (Fig. 1.1) [14]. Cby binds the C-terminal portion of β-catenin

and blocks interaction with TCF/LEF transcription factors, thus repressing β-catenin-mediated transcriptional activation [22]. Ectopic expression of Cby in 3T3-L1 cells induces spontaneous differentiation into mature adipocytes, while depletion of Cby stimulates β-catenin activity and blocks differentiation of both 3T3-L1 preadipocytes and mouse embryonic stem cells [14]. In harmony with these findings, another inhibitor of Wnt/β-catenin signaling, Dickkopf-1, is transiently expressed during human adipogenesis, and promotes differentiation of 3T3-L1 cells (Fig. 1.1) [16].

In Vivo

In accordance with its expression during adipogenesis *in vitro*, Wnt10b is highly expressed in stromal vascular cells, which are enriched for preadipocytes, but not in mature adipocytes. While there is no evidence that a deficiency of Wnt10b in mice alters adipose tissue development, overexpression of Wnt10b in adipose tissues causes a 50% reduction in adiposity under standard laboratory conditions [9], and these mice resist expansion of adipose tissue under conditions of diet-induced and genetic obesity [9,10]. Mice expressing the Wnt10b transgene also show improved glucose homeostasis and increased insulin sensitivity [9,10]. Interestingly, expression of Wnt10b either blocks brown adipose tissue development, or stimulates its conversion to white adipose tissue, depending upon promoter usage [9,23].

Regulated expression of endogenous inhibitors of Wnt signaling may also be important for modulating Wnt activity *in vivo*. For example, expression of

secreted frizzled-related protein (SFRP) 2, a putative extracellular Wnt inhibitor, is elevated in visceral adipose tissue compared to subcutaneous depots [24]. Two additional inhibitors of the Wnt pathway, SFRP5 and naked1, were recently found to be expressed in mature adipocytes and are positively correlated with increasing adiposity (Fig. 1.1) [25]. Furthermore, male mice deficient in SFRP1 show a 22% decrease in percent body fat [26] while elevated levels of SFRP1 are observed in individuals that display enhanced orbital adipogenesis associated with Graves' ophthalmopathy [27]. More research is needed to determine mechanisms by which SFRPs function in adipose tissue biology as recent studies suggest that these factors may also have functions independent of Wnt inhibition [28-30].

Wnt/β-catenin Signaling and Human Metabolic Disorders.

The importance of Wnt signaling in human health is illustrated by recent genetic research implicating members of the Wnt/β-catenin pathway in metabolic diseases. For example, polymorphisms of the *Wnt10b* and *LRP5* genes may be associated with obesity in populations of European origin [31,32] while a mutation in *LRP6* has been correlated with early coronary disease and multiple metabolic risk factors, including hyperlipidemia [33]. Furthermore, *Wnt5b* and transcription factor 7-like 2 (*TCF7L2*; formerly *TCF4*) variants have been linked to type 2 diabetes in ethnically diverse populations [19,34]. Following the initial report in which Grant *et al.* identified a link between *TCF7L2* polymorphisms and susceptibility to type 2 diabetes in Icelandic, Danish, and U.S. cohorts [34], a

number of studies were subsequently conducted that confirmed and extended this finding. Cohorts analyzed in the U.K., Finland, France, and Sweden demonstrated that variation in the *TCF7L2* genomic region does indeed affect the risk for developing type 2 diabetes in these populations [35-38]. Within the U.S., polymorphisms in *TCF7L2* were found to be associated with type 2 diabetes in large cohorts of both men and women across different ethnic backgrounds [39-41]. The mechanism by which the *TCF7L2* gene is related to risk of type 2 diabetes remains unknown. However, because Wnt signals through *TCF7L2* to activate glucagon-like peptide 1 [42], a putative mechanism in which altered levels of glucagon-like peptide 1 influence insulin secretion from pancreatic β-cells has been proposed [34]. Indeed, the reduction of insulin secretion observed in individuals harboring these polymorphisms is consistent with this hypothesis [43]. Additional studies will be required to determine the precise role of altered Wnt signaling in the pathogenesis of type 2 diabetes and other metabolic disorders, and to establish whether primary defects in adipose tissue are involved.

Recent Advances in Wnt/β-catenin-Mediated Effects on Adipogenesis

Regulation of Mesenchymal Cell Fate

Current research is focused on delineating mechanisms by which Wnt signaling influences developmental and physiological processes, with considerable progress made on the role of Wnt signaling in mesenchymal stem cells. Multipotent precursors of the mesenchymal lineage possess the ability to

differentiate into various cell types including osteoblasts and adipocytes [44]. In these cells, activation of Wnt/β-catenin signaling stimulates osteoblastogenesis and inhibits adipogenesis by modulating the relative levels of cell type specific transcription factors [45]. While early reports indicated that Wnt signaling prevents induction of the master adipogenic regulators C/EBPα and PPARγ during preadipocyte differentiation, recent research demonstrates that transient activation of Wnt/β-catenin signaling rapidly suppresses these factors in bipotential ST2 cells, and that this suppression precedes the Wnt-induced increase in osteoblastogenic transcription factors [46]. Thus, while expression of inhibitory Wnts does not influence induction of the early adipogenic factors C/EBPβ or C/EBPδ [7,45,46], repression of C/EBPα and PPARγ appears to be a primary mechanism by which Wnt signaling controls mesenchymal cell fate. Farmer and colleagues have observed an additional relationship between β-catenin and PPARγ in which these two factors functionally interact to negatively regulate each other's activity (Fig. 1.1) [47,48].

Wnt/β-catenin signaling has also been implicated in the balance between adipogenesis and myogenesis. Specifically, loss of Wnt10b *in vivo* owing to aging or targeted deletion leads to increased adipogenic potential of myoblasts and the acquisition of adipocyte characteristics during muscle regeneration [49,50]. Furthermore, conditional deletion of β-catenin in the developing mouse myometrium results in its conversion to adipose tissue [13], providing compelling evidence that the Wnt/β-catenin pathway is an important regulator of adipogenesis and mesenchymal cell fate *in vivo*.

β-catenin as a Central Mechanism for Inhibiting Adipogenesis

Although β-catenin was initially thought to function exclusively as a Wnt effector, it is now clear that binding occurs between β-catenin and signaling factors in other pathways, and that these interactions are important for cellular processes including adipogenesis. For example, Cawthorn *et al.* demonstrated that suppression of C/EBPα and PPARγ by TNFα coincides with enhanced expression of several downstream targets of Wnt/β-catenin signaling (Fig. 1.1) [51]. Indeed, the authors reported that TCF7L2-dependent transcriptional activity is enhanced and β-catenin is stabilized during inhibition of adipogenesis by TNFα. Although stabilization of β-catenin still occurred, expression of dominant-negative TCF7L2 completely blocked the inhibition of adipogenesis by TNFα, providing further support for downstream effectors of the Wnt pathway mediating cytokine-induced inhibition of differentiation [51,52].

Additional evidence of a central role for the Wnt/β-catenin pathway in adipogenesis comes from studies on liganded nuclear receptors. In response to testosterone, androgen receptor binds β-catenin and shuttles it into the nucleus where it interacts with TCF/LEF transcription factors to inhibit adipogenesis (Fig. 1.1) [53]. A distinct mechanism exists for the vitamin D receptor, which inhibits adipogenesis in bone marrow stromal cells at least in part by suppressing the expression of dickkopf-1 and SFRP2, secreted inhibitors of Wnt/β-catenin signaling [54]. Thus diverse signaling mechanisms converge on the Wnt/β-catenin pathway directly through interaction with β-catenin, or indirectly through

regulated expression of factors that modulate Wnt/β-catenin signaling. These data suggest that the Wnt/β-catenin pathway represents a major axis upon which various signals converge to influence preadipocyte differentiation.

Conclusions

Since the initial report that Wnt/β-catenin signaling potently inhibits adipogenesis in cell culture models, there have been numerous advances illustrating the importance of this regulatory pathway in directing the fate of mesenchymal precursors. While progress has been made with regard to the mechanisms underlying Wnt's inhibition of adipogenesis and stimulation of osteoblastogenesis, questions remain that must be addressed to fully understand the roles of Wnt signaling in adipose tissue and bone biology. Of particular importance will be studies aimed at understanding the cascade of events that occurs following activation of TCF/LEF by β-catenin. Future experiments will provide insight into whether the Wnt/β-catenin pathway is a viable target to improve human health.

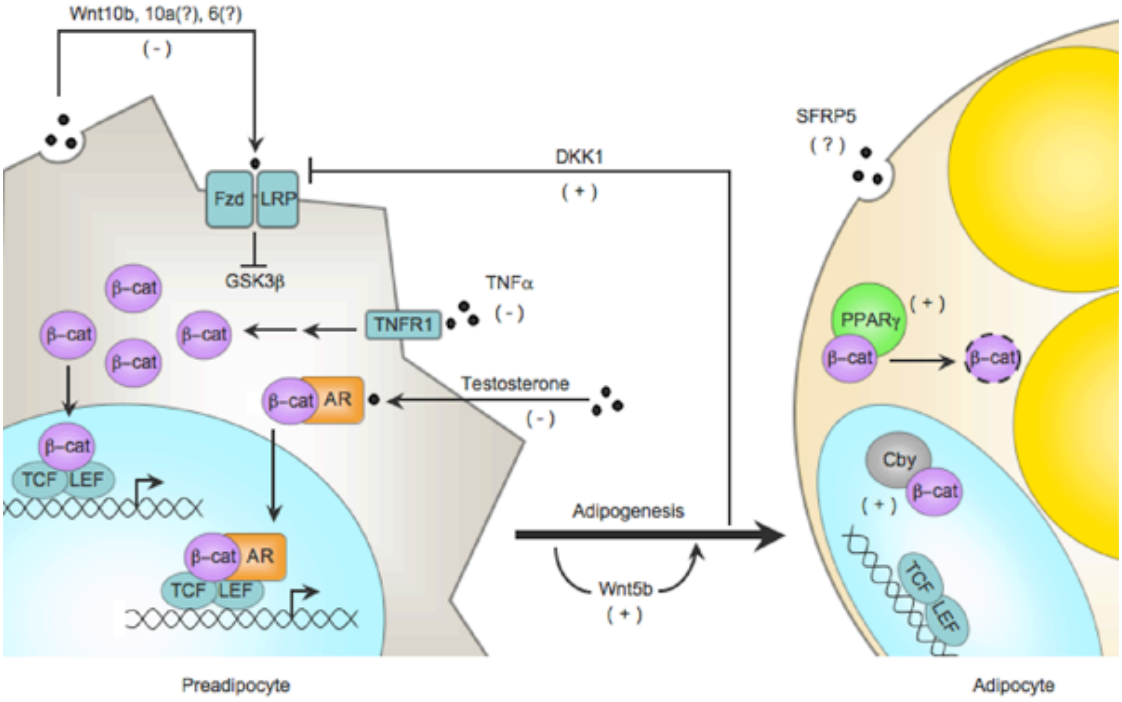

Figure 1.1. Wnt/β-catenin Signaling is a Central Pathway Regulating Adipogenesis. Wnt/β-catenin signaling in preadipocytes is initiated by expression of Wnt10b, Wnt10a, and Wnt6. Binding of these Wnts to transmembrane frizzled receptors and LRP coreceptors inhibits GSK3β leading to hypophosphorylation and stabilization of β-catenin in the cytoplasm. β-catenin is then translocated to the nucleus where it binds TCF/LEF transcription factors and activates downstream targets to inhibit preadipocyte differentiation. Factors from other inhibitory pathways converge on the Wnt/β-catenin pathway to block adipocyte conversion. TNFα signals through its receptor, TNFα receptor-1, to stabilize β-catenin and activate downstream pathways. Testosterone inhibits adipogenesis in part by stimulating interactions between androgen receptor and β-catenin. This complex travels to the nucleus to promote β-catenin-mediated gene transcription. DKK1 and Wnt5b are transiently induced during adipogenesis and stimulate preadipocyte differentiation. DKK1 prevents Wnt signaling by inhibiting LRP coreceptors, while Wnt5b promotes differentiation through an unknown mechanism. As adipogenesis proceeds, the expression of another Wnt inhibitor, Cby, is induced. Cby binds β-catenin in the nucleus and prevents coactivation of TCF/LEF transcription factors. Finally, binding of β-catenin to PPARγ leads to rapid degradation of β-catenin through a mechanism that involves the proteosome. (-) indicates factors that inhibit preadipocyte differentiation and (+) denotes factors that stimulate the process.

References

1. Rosen ED, Walkey CJ, Puigserver P, Spiegelman BM: **Transcriptional regulation of adipogenesis**. *Genes Dev* 2000, **14**:1293-1307.

2. Farmer SR: **Transcriptional control of adipocyte formation**. *Cell Metab* 2006, **4**:263-273.

3. Rosen ED, MacDougald OA: **Adipocyte differentiation from the inside out**. *Nat Rev Mol Cell Biol* 2006, **7**:885-896.

4. Wu Z, Rosen ED, Brun R, Hauser S, Adelmant G, Troy AE, McKeon C, Darlington GJ, Spiegelman BM: **Cross-regulation of C/EBP alpha and PPAR gamma controls the transcriptional pathway of adipogenesis and insulin sensitivity**. *Mol Cell* 1999, **3**:151-158.

5. Logan CY, Nusse R: **The Wnt signaling pathway in development and disease**. *Annu Rev Cell Dev Biol* 2004, **20**:781-810.

6. Clevers H: **Wnt/beta-catenin signaling in development and disease**. *Cell* 2006, **127**:469-480.

7. Ross SE, Hemati N, Longo KA, Bennett CN, Lucas PC, Erickson RL, MacDougald OA: **Inhibition of adipogenesis by Wnt signaling**. *Science* 2000, **289**:950-953.

8. Bennett CN, Ross SE, Longo KA, Bajnok L, Hemati N, Johnson KW, Harrison SD, MacDougald OA: **Regulation of Wnt signaling during adipogenesis**. *J Biol Chem* 2002, **277**:30998-31004.

9. Longo KA, Wright WS, Kang S, Gerin I, Chiang SH, Lucas PC, Opp MR, MacDougald OA: **Wnt10b inhibits development of white and brown adipose tissues**. *J Biol Chem* 2004, **279**:35503-35509.

10. Wright WS, Longo KA, Dolinsky VW, Gerin I, Kang S, Bennett CN, Chiang SH, Prestwich TC, Gress C, Burant CF, et al.: **Wnt10b inhibits obesity in ob/ob and agouti mice**. *Diabetes* 2007, **56**:295-303.

11. Moldes M, Zuo Y, Morrison RF, Silva D, Park BH, Liu J, Farmer SR: **Peroxisome-proliferator-activated receptor gamma suppresses Wnt/beta-catenin signalling during adipogenesis**. *Biochem J* 2003, **376**:607-613.

12. Kennell JA, MacDougald OA: **Wnt signaling inhibits adipogenesis through beta-catenin-dependent and -independent mechanisms**. *J Biol Chem* 2005, **280**:24004-24010.

13. Arango NA, Szotek PP, Manganaro TF, Oliva E, Donahoe PK, Teixeira J: **Conditional deletion of beta-catenin in the mesenchyme of the developing mouse uterus results in a switch to adipogenesis in the myometrium**. *Dev Biol* 2005, **288**:276-283.

14. Li FQ, Singh AM, Mofunanya A, Love D, Terada N, Moon RT, Takemaru K: **Chibby promotes adipocyte differentiation through inhibition of beta-catenin signaling**. *Mol Cell Biol* 2007, **27**:4347-4354.

15. Waki H, Park KW, Mitro N, Pei L, Damoiseaux R, Wilpitz DC, Reue K, Saez E, Tontonoz P: **The small molecule harmine is an antidiabetic cell-type-specific regulator of PPARgamma expression**. *Cell Metab* 2007, **5**:357-370.

16. Christodoulides C, Laudes M, Cawthorn WP, Schinner S, Soos M, O'Rahilly S, Sethi JK, Vidal-Puig A: **The Wnt antagonist Dickkopf-1 and its receptors are coordinately regulated during early human adipogenesis**. *J Cell Sci* 2006, **119**:2613-2620.

17. Tseng YH, Kriauciunas KM, Kokkotou E, Kahn CR: **Differential roles of insulin receptor substrates in brown adipocyte differentiation**. *Mol Cell Biol* 2004, **24**:1918-1929.

18. Tseng YH, Butte AJ, Kokkotou E, Yechoor VK, Taniguchi CM, Kriauciunas KM, Cypess AM, Niinobe M, Yoshikawa K, Patti ME, et al.: **Prediction of preadipocyte differentiation by gene expression reveals role of insulin receptor substrates and necdin**. *Nat Cell Biol* 2005, **7**:601-611.

19. Kanazawa A, Tsukada S, Sekine A, Tsunoda T, Takahashi A, Kashiwagi A, Tanaka Y, Babazono T, Matsuda M, Kaku K, et al.: **Association of the gene encoding wingless-type mammary tumor virus integration-site family member 5B (WNT5B) with type 2 diabetes**. *Am J Hum Genet* 2004, **75**:832-843.

20. Kanazawa A, Tsukada S, Kamiyama M, Yanagimoto T, Nakajima M, Maeda S: **Wnt5b partially inhibits canonical Wnt/beta-catenin signaling pathway and promotes adipogenesis in 3T3-L1 preadipocytes**. *Biochem Biophys Res Commun* 2005, **330**:505-510.

21. Ross SE, Erickson RL, Gerin I, DeRose PM, Bajnok L, Longo KA, Misek DE, Kuick R, Hanash SM, Atkins KB, et al.: **Microarray analyses during adipogenesis: understanding the effects of Wnt signaling on adipogenesis and the roles of liver X receptor alpha in adipocyte metabolism**. *Mol Cell Biol* 2002, **22**:5989-5999.

22. Takemaru K, Yamaguchi S, Lee YS, Zhang Y, Carthew RW, Moon RT: **Chibby, a nuclear beta-catenin-associated antagonist of the Wnt/Wingless pathway**. *Nature* 2003, **422**:905-909.

23. Kang S, Bajnok L, Longo KA, Petersen RK, Hansen JB, Kristiansen K, MacDougald OA: **Effects of Wnt signaling on brown adipocyte differentiation and metabolism mediated by PGC-1alpha**. *Mol Cell Biol* 2005, **25**:1272-1282.

24. Gesta S, Bluher M, Yamamoto Y, Norris AW, Berndt J, Kralisch S, Boucher J, Lewis C, Kahn CR: **Evidence for a role of developmental genes in the origin of obesity and body fat distribution**. *Proc Natl Acad Sci U S A* 2006, **103**:6676-6681.

25. Koza RA, Nikonova L, Hogan J, Rim JS, Mendoza T, Faulk C, Skaf J, Kozak LP: **Changes in gene expression foreshadow diet-induced obesity in genetically identical mice**. *PLoS Genet* 2006, **2**:e81.

26. Bodine PV, Zhao W, Kharode YP, Bex FJ, Lambert AJ, Goad MB, Gaur T, Stein GS, Lian JB, Komm BS: **The Wnt antagonist secreted frizzled-related protein-1 is a negative regulator of trabecular bone formation in adult mice**. *Mol Endocrinol* 2004, **18**:1222-1237.

27. Kumar S, Leontovich A, Coenen MJ, Bahn RS: **Gene expression profiling of orbital adipose tissue from patients with Graves' ophthalmopathy: a potential role for secreted frizzled-related protein-1 in orbital adipogenesis**. *J Clin Endocrinol Metab* 2005, **90**:4730-4735.

28. Lee JL, Lin CT, Chueh LL, Chang CJ: **Autocrine/paracrine secreted Frizzled-related protein 2 induces cellular resistance to apoptosis: a possible mechanism of mammary tumorigenesis**. *J Biol Chem* 2004, **279**:14602-14609.

29. Rodriguez J, Esteve P, Weinl C, Ruiz JM, Fermin Y, Trousse F, Dwivedy A, Holt C, Bovolenta P: **SFRP1 regulates the growth of retinal ganglion cell axons through the Fz2 receptor**. *Nat Neurosci* 2005, **8**:1301-1309.

30. Lee HX, Ambrosio AL, Reversade B, De Robertis EM: **Embryonic dorsal-ventral signaling: secreted frizzled-related proteins as inhibitors of tolloid proteinases**. *Cell* 2006, **124**:147-159.

31. Christodoulides C, Scarda A, Granzotto M, Milan G, Dalla Nora E, Keogh J, De Pergola G, Stirling H, Pannacciulli N, Sethi JK, et al.: **WNT10B mutations in human obesity**. *Diabetologia* 2006, **49**:678-684.

32. Guo YF, Xiong DH, Shen H, Zhao LJ, Xiao P, Guo Y, Wang W, Yang TL, Recker RR, Deng HW: **Polymorphisms of the low-density lipoprotein receptor-related protein 5 (LRP5) gene are associated with obesity phenotypes in a large family-based association study**. *J Med Genet* 2006, **43**:798-803.

33. Mani A, Radhakrishnan J, Wang H, Mani A, Mani MA, Nelson-Williams C, Carew KS, Mane S, Najmabadi H, Wu D, et al.: **LRP6 mutation in a family with early coronary disease and metabolic risk factors**. *Science* 2007, **315**:1278-1282.

34. Grant SF, Thorleifsson G, Reynisdottir I, Benediktsson R, Manolescu A, Sainz J, Helgason A, Stefansson H, Emilsson V, Helgadottir A, et al.: **Variant of transcription factor 7-like 2 (TCF7L2) gene confers risk of type 2 diabetes**. *Nat Genet* 2006, **38**:320-323.

35. Groves CJ, Zeggini E, Minton J, Frayling TM, Weedon MN, Rayner NW, Hitman GA, Walker M, Wiltshire S, Hattersley AT, et al.: **Association analysis of 6,736 U.K. subjects provides replication and confirms TCF7L2 as a type 2 diabetes susceptibility gene with a substantial effect on individual risk**. *Diabetes* 2006, **55**:2640-2644.

36. Scott LJ, Bonnycastle LL, Willer CJ, Sprau AG, Jackson AU, Narisu N, Duren WL, Chines PS, Stringham HM, Erdos MR, et al.: **Association of transcription factor 7-like 2 (TCF7L2) variants with type 2 diabetes in a Finnish sample**. *Diabetes* 2006, **55**:2649-2653.

37. Cauchi S, Meyre D, Dina C, Choquet H, Samson C, Gallina S, Balkau B, Charpentier G, Pattou F, Stetsyuk V, et al.: **Transcription factor TCF7L2 genetic study in the French population: expression in human beta-cells and adipose tissue and strong association with type 2 diabetes**. *Diabetes* 2006, **55**:2903-2908.

38. Mayans S, Lackovic K, Lindgren P, Ruikka K, Agren A, Eliasson M, Holmberg D: **TCF7L2 polymorphisms are associated with type 2 diabetes in northern Sweden**. *Eur J Hum Genet* 2007, **15**:342-346.

39. Zhang C, Qi L, Hunter DJ, Meigs JB, Manson JE, van Dam RM, Hu FB: **Variant of transcription factor 7-like 2 (TCF7L2) gene and the risk of type 2 diabetes in large cohorts of U.S. women and men**. *Diabetes* 2006, **55**:2645-2648.

40. Damcott CM, Pollin TI, Reinhart LJ, Ott SH, Shen H, Silver KD, Mitchell BD, Shuldiner AR: **Polymorphisms in the transcription factor 7-like 2 (TCF7L2) gene are associated with type 2 diabetes in the Amish:**

replication and evidence for a role in both insulin secretion and insulin resistance. *Diabetes* 2006, **55**:2654-2659.

41. Lehman DM, Hunt KJ, Leach RJ, Hamlington J, Arya R, Abboud HE, Duggirala R, Blangero J, Goring HH, Stern MP: **Haplotypes of transcription factor 7-like 2 (TCF7L2) gene and its upstream region are associated with type 2 diabetes and age of onset in Mexican Americans**. *Diabetes* 2007, **56**:389-393.

42. Yi F, Brubaker PL, Jin T: **TCF-4 mediates cell type-specific regulation of proglucagon gene expression by beta-catenin and glycogen synthase kinase-3beta**. *J Biol Chem* 2005, **280**:1457-1464.

43. Saxena R, Gianniny L, Burtt NP, Lyssenko V, Giuducci C, Sjogren M, Florez JC, Almgren P, Isomaa B, Orho-Melander M, et al.: **Common single nucleotide polymorphisms in TCF7L2 are reproducibly associated with type 2 diabetes and reduce the insulin response to glucose in nondiabetic individuals**. *Diabetes* 2006, **55**:2890-2895.

44. Krishnan V, Bryant HU, Macdougald OA: **Regulation of bone mass by Wnt signaling**. *J Clin Invest* 2006, **116**:1202-1209.

45. Bennett CN, Longo KA, Wright WS, Suva LJ, Lane TF, Hankenson KD, MacDougald OA: **Regulation of osteoblastogenesis and bone mass by Wnt10b**. *Proc Natl Acad Sci U S A* 2005, **102**:3324-3329.

46. Kang S, Bennett CN, Gerin I, Rapp LA, Hankenson KD, Macdougald OA: **Wnt signaling stimulates osteoblastogenesis of mesenchymal precursors by suppressing CCAAT/enhancer-binding protein alpha and peroxisome proliferator-activated receptor gamma**. *J Biol Chem* 2007, **282**:14515-14524.

47. Liu J, Farmer SR: **Regulating the balance between peroxisome proliferator-activated receptor gamma and beta-catenin signaling during adipogenesis. A glycogen synthase kinase 3beta phosphorylation-defective mutant of beta-catenin inhibits expression of a subset of adipogenic genes**. *J Biol Chem* 2004, **279**:45020-45027.

48. Liu J, Wang H, Zuo Y, Farmer SR: **Functional interaction between peroxisome proliferator-activated receptor gamma and beta-catenin**. *Mol Cell Biol* 2006, **26**:5827-5837.

49. Taylor-Jones JM, McGehee RE, Rando TA, Lecka-Czernik B, Lipschitz DA, Peterson CA: **Activation of an adipogenic program in adult myoblasts with age**. *Mech Ageing Dev* 2002, **123**:649-661.

50. Vertino AM, Taylor-Jones JM, Longo KA, Bearden ED, Lane TF, McGehee RE, Jr., MacDougald OA, Peterson CA: **Wnt10b deficiency promotes coexpression of myogenic and adipogenic programs in myoblasts**. *Mol Biol Cell* 2005, **16**:2039-2048.

51. Cawthorn WP, Heyd F, Hegyi K, Sethi JK: **Tumour necrosis factor-alpha inhibits adipogenesis via a beta-catenin/TCF4(TCF7L2)-dependent pathway**. *Cell Death Differ* 2007, **14**:1361-1373.

52. Gustafson B, Smith U: **Cytokines promote Wnt signaling and inflammation and impair the normal differentiation and lipid accumulation in 3T3-L1 preadipocytes**. *J Biol Chem* 2006, **281**:9507-9516.

53. Singh R, Artaza JN, Taylor WE, Braga M, Yuan X, Gonzalez-Cadavid NF, Bhasin S: **Testosterone inhibits adipogenic differentiation in 3T3-L1 cells: nuclear translocation of androgen receptor complex with beta-catenin and T-cell factor 4 may bypass canonical Wnt signaling to down-regulate adipogenic transcription factors**. *Endocrinology* 2006, **147**:141-154.

54. Cianferotti L, Demay MB: **VDR-mediated inhibition of DKK1 and SFRP2 suppresses adipogenic differentiation of murine bone marrow stromal cells**. *J Cell Biochem* 2007, **101**:80-88.

Chapter II

A Role for sFRP5 in Adipocyte Biology and Obesity

Abstract

Research conducted over the last decade has established the Wnt/β-catenin signaling pathway as an important regulator of adipocyte differentiation. It is now known that preadipocytes secrete various Wnt proteins that act through an autocrine mechanism to inhibit preadipocyte differentiation. Further complexity arises through the regulated expression of endogenous inhibitors of Wnt/β-catenin signaling, including the family of secreted frizzled-related proteins (sFRPs). sFRPs are thought to prevent downstream Wnt signaling by binding to and sequestering Wnt molecules in the extracellular space, although recent reports have indicated sFRPs can function in roles independent of Wnt inhibition. Here we have sought to characterize a novel function for sFRP5 in adipocyte biology and obesity. We show that sFRP5 expression is strongly induced during adipocyte differentiation *in vitro* and in various models of obesity. Furthermore, sFRP5 expression is highly correlated with increasing adiposity and adipocyte size. Mice that lack functional sFRP5 resist diet-induced obesity as evidenced by lower total body weight and decreased fat mass. Detailed morphometric analysis revealed that sFRP5^{Q27stop} mice challenged with a high fat diet have proportionally fewer large adipocytes than wild type mice, and using a model of

adipose tissue transplantation we show that sFRP5 regulates adipocyte size during obesity in a tissue autonomous manner. In an attempt to elucidate the mechanism of action of sFRP5, we found that sFRP5 regulates adipocyte clustering of 3T3-L1 cells, a similar result to that observed upon activation of integrin signaling in adipocytes. Indeed, we show that sFRP5 can functionally interact with integrins in a gel contraction assay, and that activation of the integrin/ERK signaling pathway is altered in two distinct models of sFRP5-deficient adipocytes in culture. Thus we provide evidence that sFRP5 regulates adipocyte expansion during obesity, and that the integrin/ERK cascade may mediate these effects.

Introduction

Wnt signaling is a well-studied, critical component of numerous developmental and disease processes [1,2]. Despite our long-standing knowledge of this pathway's impact on biology, discovery of novel downstream effectors and targets of Wnt signaling cascades continues to occur at a rapid pace. Further complexity in the pathway arises from the identification and cloning of endogenous inhibitors of Wnt signaling, including the family of secreted frizzled-related proteins (sFRPs) [3-5]. The sFRP family consists of eight members, sFRP1-5, sizzled, sizzled2, and crescent, five of which are found in mammals (sFRP1-5) [3]. Studies aimed at characterizing sFRP function have focused on their role in modulating the Wnt pathway *in vitro* and *in vivo* and have provided evidence for direct interaction of sFRPs with Wnt ligands [6-9].

However, these interactions serve to further highlight the inherent complexity of the pathway as variable specificity and concentration dependent effects have been reported [6,7,10,11].

Support for the hypothesis that sFRPs function to suppress the Wnt pathway *in vivo* is found in a number of recent studies linking epigenetic inactivation of sFRP genes with various types of cancer [12-16]. For example, epigenetic loss of sFRP function has been shown to occur early in colorectal cancer progression, a disease in which 90% of cases are associated with mutations in Wnt pathway genes that result in increased accumulation of β-catenin in the nucleus [12,17]. Moreover, restoration of sFRP function in colorectal cancer cells attenuates Wnt signaling even in the presence of downstream mutations, indicating that epigenetic inactivation of sFRP genes results in constitutive activation of Wnt signaling and promotion of cancer [12].

While this classical role for sFRPs is well documented, it is now clear that sFRPs also function across a broader range of cellular processes that may be independent of Wnt inhibition [18]. For example, sFRP1 has been reported to directly bind and activate Frizzled receptors 2, 4, and 7 [19,20]. Interestingly, sFRP2 has been shown to bind the fibronectin-integrin-α5β1 complex to promote cell adhesion and block apoptosis [21]. Additionally, sFRP1 can inhibit osteoclast formation by interacting with RANKL, preventing it from binding to RANK [22]. Furthermore, sizzled interacts with metalloproteinases, inhibiting their activity and leading to indirect inactivation of BMP signaling [23,24]. Thus,

sFRPs appear to function in a variety of cellular events, often in concert with factors separate and distinct from known Wnt pathway components.

In the present study, we have evaluated the role of sFRP5 in adipocyte biology and obesity. Previously Koza et al. reported that sFRP5 is expressed in adipocytes and correlated with increasing weight gain [25]. Here we extend those findings to show that sFRP5 expression is induced during adipocyte differentiation and highly correlated with increasing adiposity and relative adipocyte size in multiple models of obesity. Moreover, we demonstrate that mice lacking functional sFRP5 resist diet-induced obesity and exhibit a decrease in fat mass. Using quantitative histological methods, we observed that sFRP5 regulates adipocyte size during obesity in a tissue dependent manner, thus revealing a novel role for sFRP5 in the pathology of adipose tissue. Further investigation into the mechanism of action of sFRP5 in adipocytes revealed a functional interaction between sFRP5 and integrin signaling. We found that sFRP5-mediated collagen gel contraction is dependent on functional integrin β1 and that activation of downstream effectors of the integrin/ERK pathway is altered in adipocytes lacking sFRP5. We conclude that sFRP5 plays an important role in regulating adipocyte growth during the development of obesity.

Materials and Methods

Animals

Animal care was overseen by the Unit for Laboratory Animal Medicine (University of Michigan). LXRβ -/- mice were generated by gene targeting and

have been described previously [26]. sFRP5^{Q27stop} mice were generated by ENU mutagenesis in which a C79T mutation created a premature stop codon at Gln 27, likely producing a null allele [27]. All animals were housed with a regular 12-hour light/dark cycle and were fed *ad libitum* with standard rodent chow diet (Laboratory Rodent Diet 5001, LabDiet, St. Louis, MO). Where indicated, mice received *ad libitum* access to a low fat diet (10% fat, D12450B, Research Diets New Brunswick, NJ) or a high fat diet (45% fat, D12451, Research Diets) for 6-24 weeks.

Cell Culture

Mouse 3T3-L1 preadipocytes and human embryonic kidney 293T cells were maintained in Dulbecco's modified Eagle's medium (GIBCO) containing 10% calf serum (Atlanta Biologicals) as described previously [28]. 3T3-L1 cells were induced to differentiate into adipocytes two days after confluence as described previously, using methylisobutylxanthine, dexamethasone, and insulin (MDI) [29].

eMSC Isolation and Culture

Ear mesenchymal stem cells were harvested from wild type and sFRP5^{Q27stop} mice as previously described [30]. eMSCs were maintained in 5% CO_2 and DMEM/F12 1:1 media (GIBCO) supplemented with 15% fetal bovine serum (Atlas Biologicals), Primocin antibiotics (Invivogen, San Diego, CA) and 20ng/ml recombinant bFGF (R&D Systems). To induce adipocyte differentiation,

recombinant bFGF was removed and replaced with MDI as described for 3T3-L1 cells above plus 5 μM troglitazone.

Plasmids

sFRP5 was amplified from a mouse eye cDNA library using forward and reverse primers containing 5' EcoR1 and 3' Xho1 restriction sites, respectively. For the sFRP5-myc fusion construct, the myc tag sequence was inserted immediately upstream of the Xho1 site in the reverse primer so as to be at the C terminus of the protein. The resulting amplicons were cloned into the EcoR1 and Xho1 sites of pcDNA3.1+ (Invitrogen) to generate pcDNA3.1+(sFRP5) and pcDNA3.1+(sFRP5-myc) constructs. sFRP5 and sFRP5-myc were further subcloned into the pMSCVneo retroviral vector (Clontech) using the EcoR1 and Xho1 sites for subsequent stable infection into 3T3-L1 preadipocytes.

Transfections and Infections

For sFRP5 localization studies, 293T cells were transiently transfected with pcDNA3.1+(sFRP5-myc) using a calcium phosphate coprecipitation method as previously described [31]. Retroviral infection and selection procedures were performed essentially as described [32]. Briefly, 293T cells were transfected by calcium phosphate coprecipitation as above. About 16 hours after transfection virus-containing media was collected, passed through a 0.45-μm syringe filter, and combined with polybrene (hexadimethrine bromide; Sigma-Aldrich, St. Louis, MO) to a final concentration of 8 μg/ml. This media was then applied to

subconfluent (25-40% confluent) 3T3-L1 preadipocytes. The infection protocol was repeated every 12 hours until cells were approximately 80% confluent. 3T3-L1 cells were then split 1:5 in Dulbecco's modified Eagle's medium (GIBCO) supplemented with 10% calf serum and appropriate selection agents (400 μg/ml neomycin or 2 μg/ml puromycin). Once fully selected, stably infected cells were used for the appropriate assays.

Stable Knockdown of sFRP5 in 3T3-L1 cells

Two independent methods were used to knockdown sFRP5 in 3T3-L1 cells. First, four separate shRNA constructs targeting sFRP5 were designed and cloned into the pSUPERIOR.retro.puro retroviral vector from OligoEngine (Seattle, WA) as previously described [31]. Two of these constructs, sFRP5(1) (puromycin resistant) and sFRP5(4) (neomycin resistant) were co-infected into 3T3-L1 preadipocytes to created a stable cell line that achieve ~90% knockdown of sFRP5. Co-infected cells were selected and maintained in double selection DMEM media (400 μg/ml neomycin and 2 μg/ml puromycin) supplemented with 10% calf serum. Second, four independent shRNA constructs targeting sFRP5 were purchased from OriGene (Rockville, MD). Stable infection with construct sFRP5(sh3) achieved ~85% knockdown of sFRP5 in 3T3-L1 cells compared to cells expressing the GFP control vector.

Gel Contraction

For collagen gel contraction studies, subconfluent 3T3-L1 preadipocytes were incubated with an integrin β1 blocking antibody (Ha2/5) or IgM isotype control (G235-1, BD Biosciences) for one hour. To obtain free-floating gels, 12 well culture dishes were pre-treated with 1% BSA in PBS. 3T3-L1 preadipocytes expressing sFRP5 or empty vector were trypsinized and resuspended in a type I collagen matrix (rat tail collagen type I, BD Biosciences) at a concentration of 500,000 cells/ml according to manufacturers instructions. Gels were allowed to polymerize for 30 minutes at 37°C, after which 3T3-L1 media containing blocking antibody or IgM control were added. Collagen gel contraction was monitored at various time points over a 72-hour period and quantified using ImageJ software (http://rsb.info.nih.gov/ij/). Percent contraction was quantified by dividing the area of the contracted gel by the area of the well and expressed as a percent.

Localization of sFRP5

Separation of whole cell, ECM, and conditioned media fractions was performed based on the method of Lee [21]. Briefly, 293T cells were treated with or without 10 μg/ml heparin (Sigma-Aldrich, St. Louis, MO) for 4-6 hours. Subsequently, conditioned media were concentrated by centrifuging at 3000 x *g* for 15 min using Centriprep filter devices (Millipore, Billerica, MA). Confluent cells were then released from the culture dishes by incubating with 5 mM EDTA in PBS. The remaining ECM components were washed with PBS and extracted with Western lysis buffer (1% SDS, 60 mM Tris pH 6.8, and protease inhibitors).

Immunoblotting

Protein concentrations were determined using Protein Assay Solution (Bio-Rad, Hercules, CA). Proteins were separated by SDS-PAGE and transferred to nitrocellulose membranes. Immunoblotting was performed essentially as described [32] using anti-Myc-horseradish peroxidase (Invitrogen), p-FAK, p-ERK1/2, total ERK1/2 (Cell Signaling) antibodies.

Adipocyte Isolation

Isolation of preadipocyte-containing stromal vascular and adipocyte fractions was performed as previously described [33,34].

Quantitative RT-PCR

Total RNA from adipose tissue or 3T3-L1 cells was extracted using RNA Stat60 (Tel-Test, Friendswood, TX) and then purified using RNeasy mini-kits (Qiagen, Valencia, CA). cDNA was synthesized using the TaqMan system (Applied Biosystems, Foster, CA) and random hexamer primers. Quantitative PCR was performed according to the manufacturer's protocol. SYBR Green I was used to monitor amplification of DNA on the iCycler and IQ real-time PCR detection system (Bio-Rad Laboratories). Gene expression was normalized to cyclophilin mRNA or 18S rRNA levels as indicated.

Dual Energy X-ray Absorptiometry

Wild type and sFRP5^{Q27stop} mice were anesthetized using inhaled isoflurane and scanned using the PIXImus2 Mouse Densitometer (GE Medical Systems, Madison, WI). System software estimated fat mass, lean mass, and bone mineral content for each mouse.

Blood Chemistry

Whole blood was collected from the saphenous vein of random fed wild type and sFRP5^{Q27stop} mice on either a normal chow or high fat diet. Plasma was then prepared and stored at –80°C until assayed. Insulin, leptin, and other adipokines were simultaneously measured on a Luminex 100 machine using the Lincoplex mouse serum adipokine kit according to the manufacturer's protocol (Linco Research, St. Charles, MO).

Glucose Tolerance Test

To test glucose tolerance, wild type and sFRP5^{Q27stop} mice were given an intraperitoneal injection of 1.5 mg glucose/g body weight after a 12-hour fast. Blood glucose was determined at the indicated times from tail blood using the OneTouch Ultra glucometer (Lifescan, Burnaby, Canada).

Adipocyte Histology

Gonadal white adipose tissue was dissected from wild type and sFRP5^{Q27stop} mice that had received transcardial perfusions with 4% paraformaldehyde. The tissue was maintained in additional fixative for 24 hours.

After embedding in paraffin, adipose tissue sections were stained with hematoxylin and eosin. Images were taken on an Olympus BX-51 microscope with an Olympus DP70 color digital camera. Adobe Photoshop was used to enhance the contrast of the images before analysis. Integrated morphometry analysis was used to calculate cellular cross sectional area and the number of adipocytes per field using MetaMorph software (version 6.1; Molecular Devices, Downingtown, PA).

Adipose Tissue Transplantation

Gonadal while adipose tissue was excised from wild type and sFRP5^{Q27stop} donor mice and transplanted subcutaneously into *db/db* recipient mice at four weeks of age. To control for host differences in hyperphagia, vasculature formation, or other variables, 100 mg pieces of tissue from two wild type and two sFRP5^{Q27stop} mice were transplanted into the same *db/db* recipient. After 10 weeks, the transplanted tissue was harvested and fixed in 4% paraformaldehyde for 24 hours. Hematoxylin and eosin stained sections were subjected to morphometric analysis as described above.

Food Intake

Mice on a high fat diet were housed individually in microisolator cages and acclimated for at least seven days. Food consumption was measured every other day for one week.

Fecal Lipid Content

Fecal pellets were collected and frozen (-20^{o}C) until analysis. For the analysis of fecal lipid, pellets were put in pre-weighed tins, and heated at 60^{o}C for up to 2 hours, or until dry weight was reached. The pellets were crushed into a fine powder with a mortar and pestle. Fecal lipid was extracted according to the method of Folch [35]. Briefly, one gram of fecal powder was gently mixed overnight using 10 ml of chloroform:methanol (v:v, 2:1). The following day, the tube contents were gravity filtered (Whatman no. 1) and rinsed with 3 ml of fresh chloroform:methanol (v:v, 2:1). We added 1 ml sterile H_2O to the collected solvent, then mixed the tubes vigorously and allowed them to sit overnight to permit layer separation. The following day, the top water layer was carefully removed, and the organic layer containing lipid was added to a pre-weighed tin. The chloroform and methanol were then allowed to volatilize and the remaining lipid was quantified by weighing.

Metabolic Profiling

After acclimating to the appropriate conditions for one week, oxygen consumption, carbon dioxide production, respiratory quotient, and activity were measured in wild type and sFRP5^{Q27stop} mice using a comprehensive lab animal monitoring system at the Michigan Metabolomics and Obesity Center at the University of Michigan. Readings were taken for three days. VO_2 and VCO_2 data were normalized to lean body mass.

Results

Expression and Localization of sFRP5 *In Vitro* and *In Vivo*

To determine whether sFRPs are regulated during adipogenesis, we analyzed expression of sFRP1-5 during a time course of 3T3-L1 preadipocyte differentiation. We found that two members of the sFRP family, sFRP2 and sFRP5, showed dynamic expression patterns. sFRP2 mRNA is expressed at maximal levels in confluent preadipocytes then rapidly downregulated upon induction of adipogenesis. Conversely, sFRP5 mRNA expression is induced during adipogenesis, reaching maximal expression six days after initiation of differentiation (Figure 2.1a). Consistent with our *in vitro* findings and in agreement with published reports, sFRP5 mRNA is expressed predominantly in the adipocyte fraction of adipose tissue (Figure 2.1b) [25].

sFRP1 and sFRP2 are thought to act locally by remaining tightly associated with the extracellular matrix (ECM) [6,21]. To determine whether sFRP5 exhibits similar extracellular localization, 293T cells were transiently transfected with pcDNA3.1+ vector or vector expressing an sFRP5-myc fusion protein. To achieve separation of whole cell and ECM fractions, transfected cells were treated with 5 mM EDTA to detach cells from the culture dish without destroying the underlying ECM. Whole cell, ECM, and conditioned media fractions were collected and subjected to immunoblot analysis. sFRP5 protein was detected in the whole cell and ECM fractions but not in the conditioned media (Figure 2.1c). In agreement with previous studies on sFRP1 localization [6], sFRP5 is liberated from the ECM by addition of exogenous heparin and can

subsequently be detected in the conditioned media (Figure 2.1c). Similar results are also observed in 3T3-L1 adipocytes stably expressing sFRP5 (data not shown). These data suggest that upon secretion from the cell, sFRP5 is incorporated into the ECM and likely functions in an autocrine or paracrine manner.

sFRP5 is Associated with Increasing Adiposity and Adipocyte Size

To determine whether sFRP5 expression is altered during obesity, we evaluated sFRP5 mRNA levels across a range of diet-induced and genetically obese mouse models. Quantitative RT-PCR analysis of RNA from white adipose tissue of C57BL/6J mice fed either a low fat or a high fat diet for six months revealed that sFRP5 expression is increased 25 fold in high fat-fed mice (Figure 2.2d). sFRP5 levels are also increased in white adipose tissue from leptin-deficient *ob/ob* mice [eight fold] (data not shown) and in mice that have become obese following ovariectomy (Figure 2.2b). sFRP5 expression displays a strong positive correlation with percent body fat in high fat diet (R^2=0.8426) and ovariectomized models (R^2=0.7579), (Figure 2.2a,b). In contrast, sFRP2 expression is neither increased during obesity nor correlated with increasing adiposity (Figure 2.2a). Thus sFRP5 is specifically upregulated during obesity and displays a strong correlation with increasing adiposity.

As obesity is characterized in part by adipocyte hypertrophy, we sought to examine the relationship between sFRP5 expression and adipocyte size. We analyzed histological sections of white adipose tissue from C57BL/6J mice

challenged with a high fat diet and found that adipocytes from these mice were approximately two times larger than those from mice fed a low fat diet (data not shown). When sFRP5 expression was compared with relative adipocyte size, we found that the two variables were highly correlated (Figure 2.2c). Leptin, which is known to be increased in relation to adipocyte size, and sFRP2 are also shown for comparison (Figure 2.2c).

Finally, we examined sFRP5 expression in adipose tissue from LXRβ -/- mice, as adipocytes from these mice do not undergo diet-induced hypertrophy. Importantly, we found that sFRP5 expression was not increased in LXRβ -/- mice challenged with a high fat diet (Figure 2.2d). Taken together, the results of these studies suggest a strong positive relationship between sFRP5 expression and adipocyte size.

sFRP5^{Q27stop} Mice Resist Diet-Induced Obesity and Display a Reduction in Fat Mass

To evaluate the role of sFRP5 in adipocyte biology and obesity *in vivo*, we obtained sFRP5^{Q27stop} mice that were generated by ENU mutagenesis in which a single base pair mutation resulted in a premature stop codon at glutamine 27, likely creating a nonfunctional allele (Figure 2.3a) [27].

sFRP5^{Q27stop} mice are indistinguishable from wild type mice under standard chow-fed conditions as assessed by total body weight, body composition, tissue weights, metabolic phenotyping [plasma insulin, VO_2, VCO_2, respiratory quotient], and analysis of secreted adipokines [leptin and resistin]

(data not shown). Therefore, we sought to investigate the role of sFRP5 in obesity by challenging 12-16 week old sFRP5^{Q27stop} mice with a high fat diet. We found that sFRP5^{Q27stop} mice resist diet-induced weight gain compared to high fat-fed wild type mice (Figure 2.3b). Analysis of body composition by Dual Energy X-Ray Absorptiometry (DEXA) revealed that the difference in total body weight is due solely to a decrease in fat mass in sFRP5^{Q27stop} mice, as lean mass, bone mineral content, and organ weights are nearly identical between genotypes (Figure 2.3c, data not shown). Consequently, sFRP5^{Q27stop} mice have a lower percent body fat compared to controls (Figure 2.3d). Furthermore, analysis of random fed blood variables by ELISA revealed that plasma leptin and plasma insulin are decreased in sFRP5^{Q27stop} mice compared to wild type controls (Figure 2.3e). These differences presumably reflect an increase in leptin and insulin resistance in the obese wild type mice, and also serve as further evidence of decreased fat mass in sFRP5^{Q27stop} mice.

To determine whether glucose homeostasis was altered in sFRP5^{Q27stop} mice, we performed a glucose tolerance test. High fat-fed wild type and sFRP5^{Q27stop} mice were fasted for 12 hours, after which glucose was injected intraperitoneally. There were no significant differences in fasted blood glucose or glucose tolerance in sFRP5^{Q27stop} mice (Figure 2.3f). While sFRP5^{Q27stop} mice are able to clear glucose to the same extent as wild type mice, lower levels of plasma insulin in fed mice suggest that sFRP5^{Q27stop} mice are more insulin sensitive than wild type mice.

Taken together, these results show that sFRP5^{Q27stop} mice resist diet-induced weight gain and that this effect is due to alterations in fat mass.

sFRP5 Regulates Adipocyte Size During Obesity in a Tissue Autonomous Manner

Based on our previous findings that sFRP5 mRNA expression is highly correlated with increasing adipocyte size (Figure 2.2c,d), we hypothesized that the observed decrease in fat mass in sFRP5^{Q27stop} mice on a high fat diet would be associated with alterations in adipocyte hypertrophy. To test this hypothesis we performed histological analyses on gonadal white adipose tissue (G-WAT) from wild type and sFRP5^{Q27stop} mice that had been challenged with a high fat diet for six weeks. In agreement with our previous observations of body composition using DEXA, we found that G-WAT from sFRP5^{Q27stop} mice weighed less than G-WAT from wild type mice (Figure 2.4a). In order to obtain a more comprehensive histological view of gonadal adipose tissue in these mice, we divided the tissue into four separate quadrants, with quadrant 1 being most proximal to the epididymis and quadrant 4 the most distal section of tissue (Figure 2.4b).

While our earlier analysis of relative adipocyte size was determined by quantifying the number of adipocytes in a given microscopic field, we wished to obtain a more accurate representation of adipocyte cross-sectional area. Using MetaMorph software (Molecular Devices) we were able to precisely calculate adipocyte size from hematoxylin and eosin stained sections of G-WAT from wild

type and sFRP5^{Q27stop} mice. This analysis revealed that there were proportionally fewer large adipocytes in sFRP5^{Q27stop} G-WAT compared to controls, with the 53% difference between wild type and sFRP5^{Q27stop} adipocytes in quadrant 3 being statistically significant (Figure 2.4c). Here we define large adipocytes as cells greater than 8000 μm^2. These large adipocytes, while rarely seen under standard chow-fed conditions, make up a substantial percentage of the adipose tissue volume under conditions of obesity. Thus, the differences observed here are likely to have a significant effect on the overall volume and weight of the adipose tissue of wild type and sFRP5^{Q27stop} mice.

Another observation stemming from our histological analysis involved the frequency with which crown-like structures (CLS) were seen in wild type and sFRP5^{Q27stop} mice. The term CLS is used to describe a ring or crown of macrophages surrounding a single adipocyte. These macrophages are thought to consume dead or dying adipocytes and are a marker of macrophage infiltration and inflammation associated with obesity [36]. Interestingly, we found fewer CLS in G-WAT from sFRP5^{Q27stop} mice compared to wild type controls, with the difference in quadrant 3 again being statistically significant, and trending toward significance in quadrant 4 (Figure 2.4d). These findings provide some evidence to suggest that obesity-associated inflammation and macrophage infiltration may be decreased in sFRP5^{Q27stop} mice compared with controls.

To investigate whether alterations in adipocyte size in sFRP5^{Q27stop} mice were tissue autonomous or simply a reflection of the overall adiposity of the animal, we performed an adipose tissue transplant experiment. G-WAT from

wild type and sFRP5^{Q27stop} mice was dissected and transplanted subcutaneously into *db/db* recipient mice at four weeks of age (Figure 2.4e). The contralateral G-WAT depot was also dissected and used as a baseline standard in subsequent histological analyses. As expected, the *db/db* recipient mice rapidly became obese and induced hypertrophy of adipocytes in the newly vascularized transplanted tissue. Ten weeks after transplantation, the donor tissue was excised and subjected to histological processing and MetaMorph analysis. Consistent with previous data, the results of this experiment revealed a 30% decrease in the proportion of large adipocytes in sFRP5^{Q27stop} G-WAT compared to wild type controls, whereas there were virtually no cells greater than 8000 μm^2 in either wild type or sFRP5^{Q27stop} G-WAT before transplantation (Figure 2.4f). Thus, we conclude that loss of sFRP5 limits the ability of adipocytes to expand during obesity.

Taken together, our histological and morphometric analyses indicate that sFRP5 regulates adipocyte size during obesity in a tissue autonomous manner.

Relative Expression of Vasculature and Adipocyte Markers in sFRP5^{Q27stop} Mice

Neovascularization in adipose tissue is a critical event during development of adipose tissue and obesity, ensuring that expanding adipocytes meet their requirements for oxygen and essential nutrients [37]. Therefore, one plausible cause of resistance to adipocyte hypertrophy in sFRP5^{Q27stop} mice may be due to lack of formation of vascular networks needed by adipocytes undergoing

hypertrophy. To test whether there may be altered vasculature formation in sFRP5^{Q27stop} mice, we analyzed adipose tissue expression of various modulators of vasculature maturation. We found that there were no differences in expression of angiopoietin-1, a factor thought to play a crucial role in vascular remodeling in obesity [38] (Figure 2.5a). Similarly, levels of angiopoietin-2, receptor tyrosine kinases Tie-1 and Tie-2, and smooth muscle alpha actin (ACTA2) were not different in sFRP5^{Q27stop} mice compared to wild type controls (Figure 2.5a). In addition, analysis of hematoxylin and eosin stained histological sections of adipose tissue from these mice showed no change in the frequency of large vessels (data not shown). Thus, our data suggest that vascular formation is not altered in sFRP5^{Q27stop} mice and likely does not contribute to changes in adipocyte size in this model.

To test whether the degree of preadipocyte recruitment is altered in adipose tissue from sFRP5^{Q27stop} mice, we analyzed mRNA expression of adipocyte markers and found that PPARγ, KLF15, and leptin levels are all unchanged compared to wild type mice (Figure 2.5b). These data suggest that a similar level of adipogenesis occurs in both wild type and sFRP5^{Q27stop} mice.

Finally, we examined mRNA expression of sFRP1, sFRP2, and sFRP5 in adipose tissue from wild type and sFRP5^{Q27stop} mice, as these genes comprise a subgroup of sFRPs that are highly related with regard to genetic structure. Our data indicate that sFRP5 mRNA is substantially downregulated in sFRP5^{Q27stop} mice; however, we found no compensatory upregulation of sFRP1 or sFRP2 transcripts in response to an apparent lack of sFRP5 function (Figure 2.5c).

While it appears that regulation of sFRP1 and sFRP2 mRNA is unchanged in sFRP5^{Q27stop} mice, we cannot rule out the possibility that endogenous levels of one or both of these factors may be playing a functionally redundant role to that of sFRP5 in this context [8].

Metabolic Phenotype of Mice Harboring the sFRP5^{Q27stop} Mutation

In an attempt to clarify the underlying cause of obesity resistance observed in mice homozygous for the sFRP5^{Q27stop} mutation, we evaluated food intake and fat absorption in sFRP5^{Q27stop} mice. Food intake was measured in individually housed mice for one week. Our results indicate that food intake is not changed in sFRP5^{Q27stop} mice relative to their wild type counterparts (Figure 2.6a). In contrast, the total amount of fat excreted in the feces of sFRP5^{Q27stop} mice was significantly increased by approximately 10% compared to controls (Figure 2.6b). However, calculations of food intake and feed efficiency suggest that this modest increase in excreted lipid cannot account solely for the difference in fat mass and body weight seen over a five-week period in sFRP5^{Q27stop} mice (Figure 2.3b).

We next sought to characterize whether metabolic parameters were altered in sFRP5^{Q27stop} mice compared to wild type controls. Mice from both groups were acclimated to the appropriate environmental conditions and afterward subjected to various metabolic measurements in a comprehensive lab animal monitoring system (CLAMS). We found that, despite a decrease in fat mass in sFRP5^{Q27stop} mice, differences in oxygen consumption were not

observed between the two groups (Figure 2.6c). Unexpectedly, however, carbon dioxide production was significantly lower in sFRP5^{Q27stop} mice, while respiratory quotient was not altered between genotypes (Figure 2.6d,e). Activity of the mice was also measured and was not found to be different between sFRP5^{Q27stop} mice and wild type control animals (Figure 2.6f).

Though our attempts to clarify the mechanism of obesity resistance in sFRP5^{Q27stop} mice remain incomplete, the results obtained herein suggest that in general, the metabolic profile of sFRP5^{Q27stop} mice is not substantially altered compared to wild type controls.

Integrin Signaling may Mediate sFRP5-Regulated Adipocyte Clustering

To further elucidate the role of sFRP5 in adipocyte biology we turned to cell culture-based models, utilizing both well-characterized and newly established approaches. Using retroviral delivery, we enforced ectopic expression of sFRP5 in 3T3-L1 preadipocytes but failed to detect any effect on differentiation, as cells infected with pMSCV empty vector or vector driving expression of sFRP5 showed no differences in lipid accumulation or mRNA expression of adipogenic transcription factors, PPARγ and C/EBPα (data not shown). One notable difference, however, was observed after the cells had differentiated into adipocytes. Cells overexpressing sFRP5 form larger and more numerous adipocyte clusters than control cells (Figure 2.7a). Adipocyte clusters are seen under the microscope as darker regions representing multiple layers of cells.

Interestingly, using stably expressed short hairpin RNA (shRNA) molecules to inhibit sFRP5 function in 3T3-L1 cells, we observed the opposite effect. Adipocytes expressing sFRP5 at 10% of physiological levels exhibit substantially decreased adipocyte clustering (Figure 2.7a). Moreover, a thickened area of fluorescence surrounds many of the cells in the monolayer, making single cells appear even more separate and distinct (Figure 2.7a). To extend this finding, we performed an adipocyte aggregation experiment in which 3T3-L1 adipocytes expressing either a scrambled control or two shRNA molecules against sFRP5 were detached from the culture dish and re-plated on regular plastic dishes or dishes coated with ECM components (fibronectin, collagen type I, or collagen type IV). Consistent with previous results, control adipocytes readily form large aggregates upon re-plating, while sFRP5-deficient adipocytes completely fail to form aggregates, and instead adhere to the substratum as mostly single cells (Figure 2.7b). Figure 2.7 illustrates the effect of adipocytes re-plated on collagen type IV coated plates; however, similar results were obtained using uncoated or collagen type I coated plates (data not shown). Thus, our data support a role for sFRP5 in clustering of adipocytes *in vitro*, and suggest that sFRP5 may be involved in cell-cell or cell-ECM interactions.

Integrins are known to play a significant role in adhesion of cells with other cells or with the surrounding matrix [39]. Of particular interest to our study are recent results showing that integrins are required for clustering of 3T3-L1 adipocytes [40]. In light of this recent finding, we sought to determine whether the sFRP5 and integrin pathways interact utilizing a model of 3D collagen gel

contraction, which has been shown to be dependent on integrin function [41,42]. 3T3-L1 preadipocytes expressing either pMSCV empty vector or vector expressing ectopic sFRP5 were embedded in a 3D collagen gel at a concentration of 500,000 cells/ml. Gels were monitored for several days and the amount of gel contraction was calculated at various time points. The results of this study indicate that cells expressing sFRP5 are able to contract a collagen gel at a greater rate than control cells (Figure 2.7c). To determine whether this effect is mediated by integrins, we performed the same experiment in the presence or absence of an integrin β1 blocking antibody (Ha2/5). As expected, the rate at which sFRP5-expressing cells treated with IgM control antibody contracted the collagen gels was increased compared to controls. However, treatment with the integrin β1 blocking antibody abolished this effect (Figure 2.7c). Thus, the gel-contracting ability of sFRP5-expressing 3T3-L1 preadipocytes is dependent on functional integrin β1.

To explore the relationship between sFRP5 and integrin signaling in adipocytes, we analyzed the activation status of known integrin pathway components in multiple *in vitro* models where the level of endogenous sFRP5 was decreased. The integrin/ERK cascade has been reported to play a role in the adaptation of adipocyte function to changes in cell size [43]; therefore we sought to examine the activity of this pathway in our system. In 3T3-L1 cells stably expressing shRNA constructs against sFRP5, we found that ERK1/2 phosphorylation is substantially increased (Figure 2.7d). A similar result was observed in sFRP5^{Q27stop} primary ear mesenchymal stem cells (eMSCs) that

were expanded and differentiated *in vitro* (Figure 2.7d). To extend our findings, we examined the phosphorylation state of focal adhesion kinase (FAK), a primary effector of integrin signaling activated by integrin clustering at the plasma membrane. In support of a positive relationship between sFRP5 and integrins, we found that phosphorylation of FAK at tyrosine 925 was decreased in sFRP5-deficient 3T3-L1 adipocytes and sFRP5^{Q27stop} eMSCs (Figure 2.7d). Taken together, these data suggest that sFRP5 influences adipocyte clustering, and that this may involve sFRP5-mediated alterations in integrin signaling.

Discussion

Here we show that sFRP5 expression is induced during adipocyte differentiation *in vitro* and in animal models of obesity. Furthermore, sFRP5 expression is highly correlated with increasing percent body fat and adipocyte size. Mice that lack functional sFRP5 resist diet-induced obesity as evidenced by lower total body weight and decreased fat mass. Detailed histological analysis revealed that sFRP5^{Q27stop} mice challenged with a high fat diet have proportionally fewer large adipocytes than wild type mice, and using a model of adipose tissue transplantation we subsequently found that sFRP5 regulates adipocyte size during obesity in a tissue autonomous manner.

These data support a model wherein sFRP5 expression is increased in adipocytes as they expand during obesity. In this model, sFRP5 itself further influences adipocyte growth as hypertrophy occurs to facilitate increased lipid load (Figure 8a). In addition, sFRP5 may act to inhibit autocrine Wnt signaling in

surrounding preadipocytes, thus allowing for their recruitment and differentiation under conditions of increased lipid accumulation, such as obesity (Figure 8a).

We analyzed the metabolic profile of sFRP5^{Q27stop} mice in an attempt to determine the cause of obesity resistance and reduced fat mass in these animals under conditions of high fat challenge. However, our analysis of metabolic parameters in sFRP5^{Q27stop} mice yielded no substantial differences in oxygen consumption, respiratory quotient, activity, or food intake compared to wild type mice. Thus, we conclude that obesity resistance in sFRP5^{Q27stop} mice is not the result of altered whole body metabolism. We have not ruled out, however, that undetected differences in local metabolism may have significant cumulative effects on fat mass and body weight over time. Additionally, as we predict sFRP5 function to be disrupted in all tissues of sFRP5^{Q27stop} mice, it is conceivable that the observed phenotype stems from effects in other parts of the body. Our finding that sFRP5^{Q27stop} mice excrete a modest but significantly higher amount of lipid than wild type mice suggests there may be malabsorption of lipid in the gut and lends credence to this hypothesis.

While it is clear that there are multiple factors involved, further studies are needed to determine how important changes in metabolism and energy balance are to the reduction of fat mass in high fat-challenged sFRP5^{Q27stop} mice.

The finding that creation of large adipocytes is limited in sFRP5^{Q27stop} mice suggests that sFRP5 regulates adipocyte growth during obesity. While this observation provides some insight into the cause of obesity resistance in sFRP5^{Q27stop} mice, the mechanism by which sFRP5 influences the creation of

large adipocytes remains to be elucidated. Several factors could potentially be involved. As mentioned above, the expansion of adipocytes during development of obesity requires the formation of new vasculature to provide necessary nutrients and oxygen to the cells [37]. Thus, one possible mechanism involves adipocyte-derived sFRP5 signaling in a paracrine manner to recruit new vessels into the expanding adipose depot. An increasing number of reports have shown that Wnt signaling components play a central role in neovessel formation in different tissues [44,45]. Interestingly, a recent study found that sFRP1 increases the formation of new vasculature in the mouse hindlimb after an ischemic event [20]. While these findings seem to support the notion that sFRP5 may function in a similar role, to our knowledge no studies have been reported suggesting a role for Wnt signaling in neovascularization of adipose tissue during obesity. Moreover, our analysis of adipose tissue mRNA showed no differences in expression of factors involved in vasculature formation between wild type and sFRP5^{Q27stop} mice (Figure 2.5a). Additionally, there were no differences in the frequency of large vessels in adipose tissue from sFRP5^{Q27stop} mice, although we cannot rule out the possibility of altered microvasculature formation that was not detected by our methods. Thus, based on our data we conclude that sFRP5 does not influence vascularization of adipose tissue during development of obesity.

Another event that may limit the creation of large adipocytes in sFRP5^{Q27stop} mice involves remodeling of the ECM. It stands to reason that the cage-like ECM surrounding each adipocyte must be significantly remodeled to

allow the cells to expand and accumulate lipid. Indeed, studies have shown that adipocyte growth and expansion *in vivo* and in 3D cell culture conditions is severely diminished in mice and cells lacking MT1-MMP, a membrane-anchored metalloproteinase involved in collagen degradation [46]. Based on our data that sFRP5 expression is dramatically increased in relation to adipocyte size and that sFRP5 is localized to the ECM upon secretion from the cell, it is tempting to speculate that sFRP5 may be involved in breakdown and remodeling of the ECM during adipocyte hypertrophy, particularly as sizzled has been shown to interact with metalloproteinases in vertebrates [23,24]. Furthermore, sFRP5 contains a netrin (NTR) domain similar to that found in tissue inhibitors of metalloproteinases (TIMPs), which are known to regulate activity of ECM remodeling proteins [47]. Despite these intriguing parallels, we have no evidence to suggest that sFRP5 is directly involved in ECM remodeling. Future studies to test this hypothesis should focus on characterizing the activity of matrix remodeling factors, such as matrix metalloproteinases (MMPs), under conditions of altered sFRP5 expression, since mRNA expression of these factors would not necessarily be altered.

Our finding that sFRP5 can interact with the integrin/ERK pathway may shed further light on the mechanism by which adipocytes expand during obesity. While little is known with regard to classical functions of integrins in mature adipocytes, one study has provided evidence of a potentially important role by showing that several integrin signaling components are upregulated in concert with ECM factors in adipose tissue from obese human subjects [48]. Also,

Farnier et al. showed that the integrin/ERK cascade may be involved in the adaptation of cell function to increasing adipocyte size [43]. These findings are relevant to the present study as we found that sFRP5 expression was strongly correlated with increasing adiposity and adipocyte size. Additionally, our *in vitro* studies support the existence of a relationship between sFRP5 and integrin/ERK signaling, the precedence for which comes from a report by Lee et al. who showed direct and functional interaction of sFRP2 with the integrin $\alpha5\beta1$/fibronectin complex in MCF7 cells [21].

While independent evidence of a role for the integrin/ERK pathway in large adipocytes may lend credence to our findings, it is important to recognize the discrepancies between the present study and that of Farnier et al. For example, Farnier and colleagues found that ERK1/2 phosphorylation was increased upon activation of integrin $\beta1$ signaling in large adipocytes, whereas here we report an increase in phosphorylation of ERK1/2 under conditions in which we hypothesize integrin activity would be decreased (sFRP5 deficiency). These disparities may be due to differences in experimental models as our results were obtained using 3T3-L1 cells and primary eMSCs derived from C57BL/6J mice and Farnier et al. analyzed adipocytes isolated from Zucker rats. Furthermore, ERK1/2 phosphorylation states may be dependent on the particular integrin heterodimer initiating the signaling cascade. Evidence for this comes from a recent report showing ERK1/2 phosphorylation is decreased by ~50% upon overexpression of integrin $\alpha6$ in 3T3-L1 adipocytes [40], the same model we have used in our studies.

Thus, while further research is needed to fully elucidate the role of integrin signaling in adipocyte biology, we have provided evidence to suggest that integrins may be involved in mediating sFRP5-dependent effects. Based on published reports and data presented here, we hypothesize that ECM-bound sFRP5 may interact with integrins at the cell surface and influence downstream activation of the integrin/ERK cascade to regulate adipocyte function, including adipocyte growth during obesity.

We have presented evidence of a novel role for sFRP5 in adipocyte biology and obesity. Many question remain, however, that must be addressed to gain a full understanding of the mechanism of action of sFRP5. It has been reported that canonical Wnt signaling is downregulated in mature adipocytes, raising the questions of what sFRP5 may be acting on and what role sFRP5 plays at the cell surface? Future experiments testing the interaction of sFRP5 with frizzled receptors or integrin molecules expressed in adipocytes will shed light on whether sFRP5 plays a direct signaling role leading to altered adipocyte function.

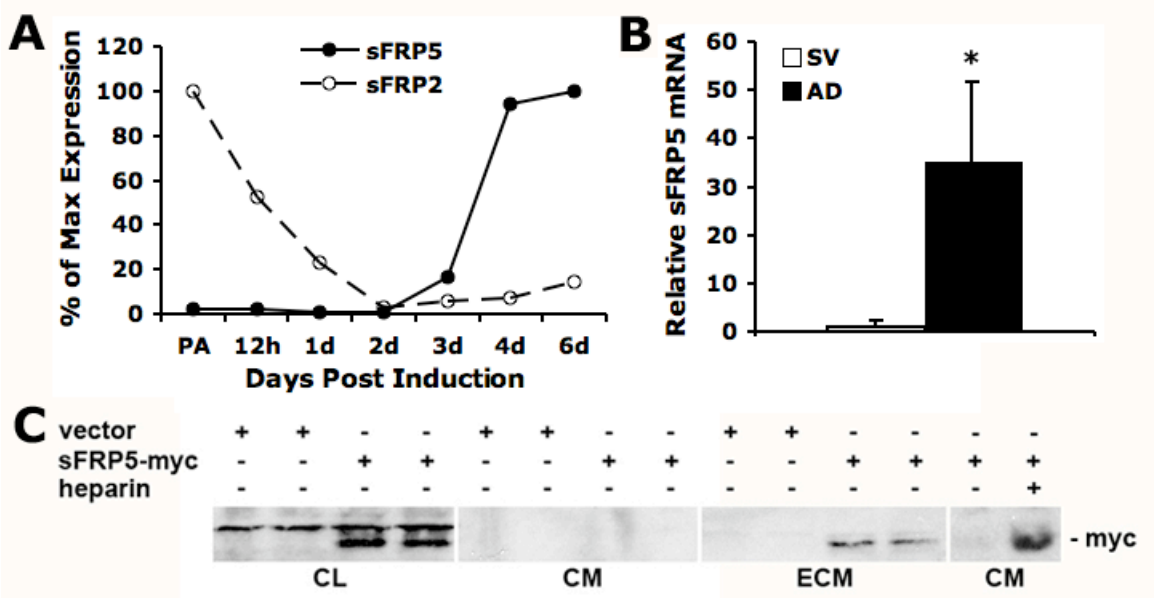

Figure 2.1. Expression and Localization of sFRP5 *In Vitro* and *In Vivo*. A, RNA was isolated from confluent 3T3-L1 cells (PA) and at the time points indicated after induction of differentiation with MDI. sFRP2 and sFRP5 transcripts were measured by quantitative RT-PCR (qPCR). All values for sFRP2 and sFRP5 are plotted as percent of maximum. **B**, White adipose tissue from B6.Cg-Ay/J mice (n=4) was separated into stromal vascular and primary adipocyte fractions by collagenase digestion. sFRP5 mRNA expression was determined by qPCR. Data are expressed as mean plus S.D. **C**, 293T cells were transiently transfected with pcDNA3.1+ empty vector or vector containing an sFRP5-myc fusion construct. sFRP5 protein is secreted but remains associated with the ECM. Upon addition of exogenous heparin (10 μg/ml), sFRP5 is released into the conditioned media. SV, stromal vascular; AD, adipocyte; CL, cell lysate; CM, conditioned media; ECM, extracellular matrix. Significance was determined using Student's t-test. *P*-values < 0.05 are depicted with an asterisk.

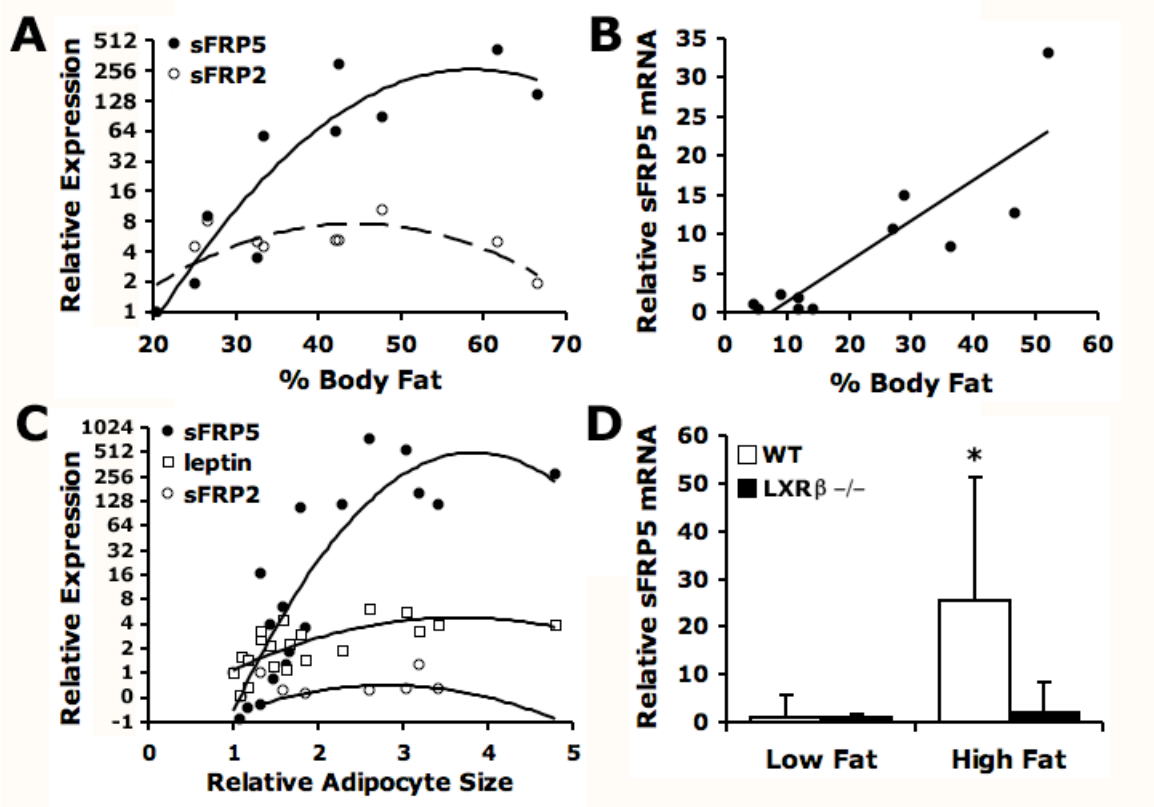

Figure 2.2. sFRP5 is Associated with Increasing Adiposity and Adipocyte Size. **A**, RNA was isolated from adipose tissue of wild type C57BL/6J mice fed either a low fat or a high fat diet for six months. A strong positive correlation is observed between relative expression of sFRP5 mRNA and percent body fat (R^2=0.8426), whereas sFRP2 mRNA expression and percent body fat do not exhibit a positive relationship. **B**, sFRP5 expression is also correlated with percent body fat in mice that became obese following ovariectomy (R^2=0.7579). **C**, Levels of sFRP5 mRNA showed a strong positive correlation with relative adipocyte size (R^2=0.7884). Relative adipocyte size was determined by comparing the number of adipocytes in a given microscopic field. Leptin (R^2=0.5141) and sFRP2 (R^2=0.1917) levels are shown for comparison. **D**, Wild type or LXRβ -/- mice were fed either a low fat or a high fat diet for six months. sFRP5 mRNA levels were measured by qPCR. Data are expressed as mean plus S.D. For all experiments, 6-10 animals per genotype were used. Significance was determined using Student's t-test. Asterisk denotes significance ($p < 0.05$) between wild type low fat versus wild type high fat.

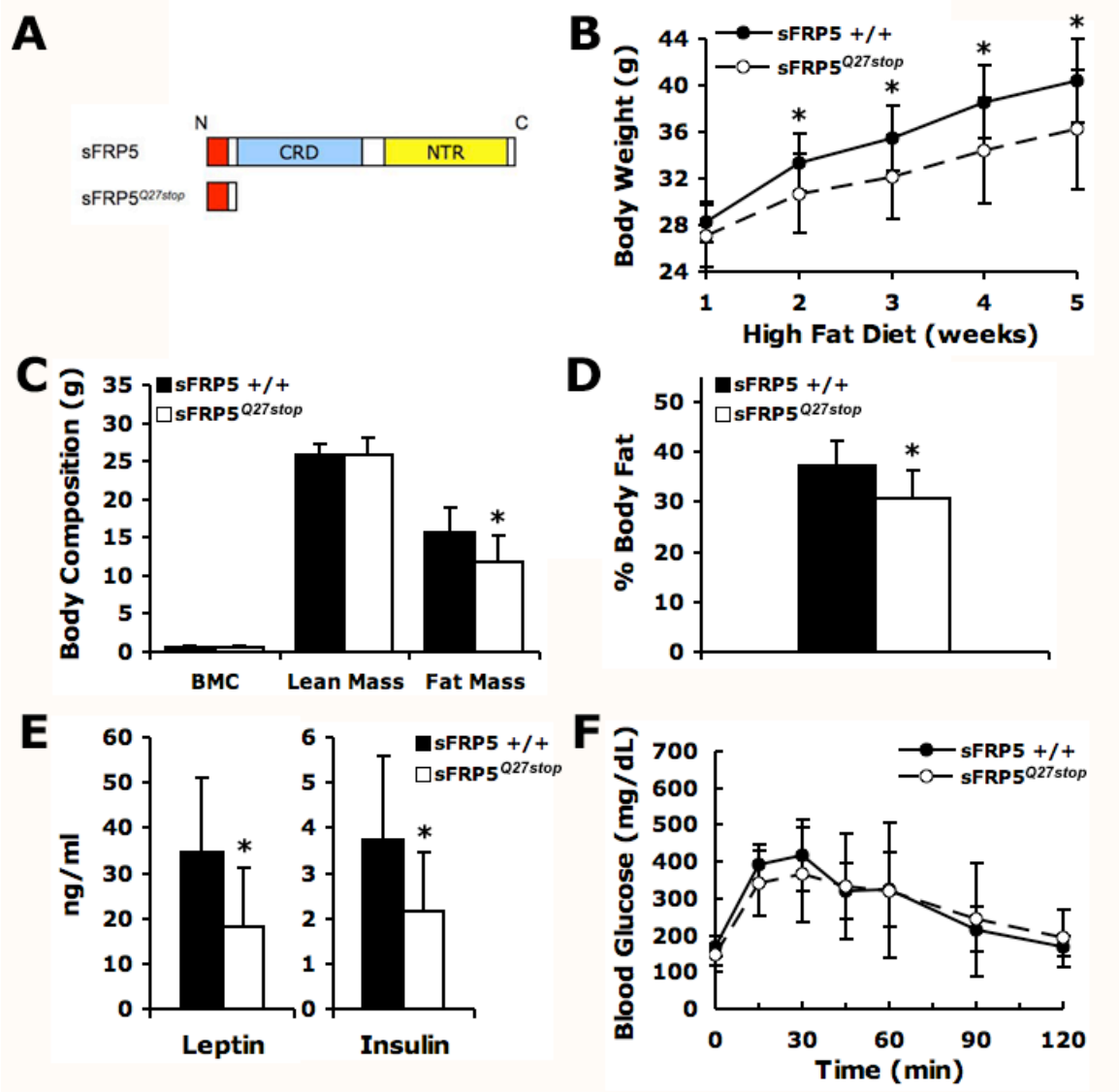

Figure 2.3. sFRP5^{Q27stop} Mice Resist Diet-Induced Obesity and Display a Reduction in Fat Mass. **A**, Diagram depicting the full-length sFRP5 protein and the predicted protein fragment in sFRP5^{Q27stop} mice. **B**, Male wild type (n=15) and sFRP5^{Q27stop} (n=14) mice were placed on a high fat diet for five weeks and total body weight was measured every week. Body weight is expressed as mean ± S.D. **C**, Body composition was determined by duel energy X-ray absorptiometry scanning in wild type and sFRP5^{Q27stop} mice. Data are expressed as mean plus S.D. **D**, Percent body fat was determined by dividing the fat mass by the total body weight and expressed as percent plus S.D. **E**, Random fed plasma leptin and insulin concentrations were detected by ELISA and expressed as mean plus S.D. **F**, Wild type and sFRP5^{Q27stop} mice were fasted for 12 hours and glucose was administered intraperitoneally. Data are expressed as mean ± S.D. BMC, bone mineral content; CRD, cysteine rich domain; NTR, netrin domain. Significance was determined using Student's t-test. *P*-values < 0.05 are depicted with an asterisk.

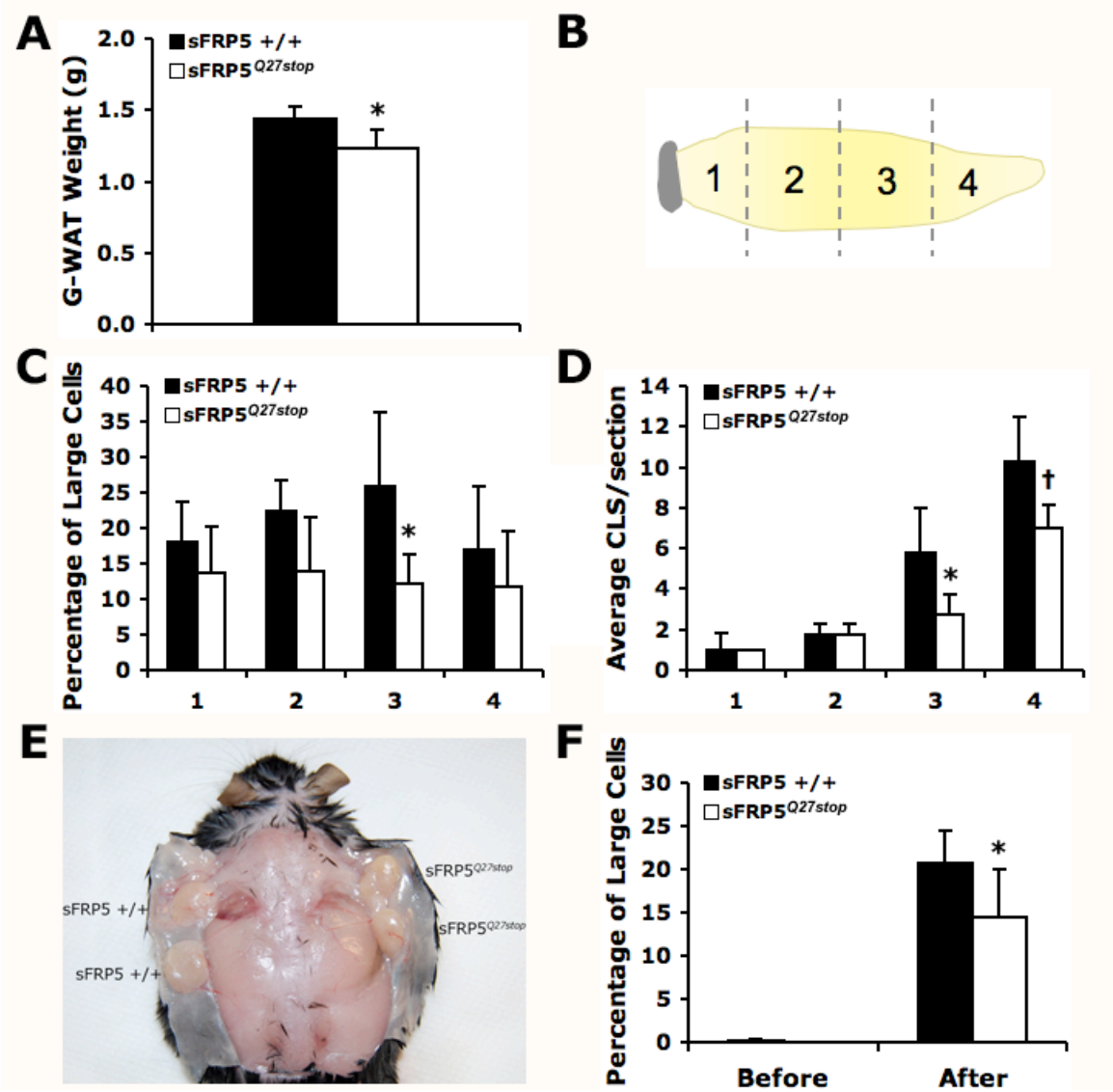

Figure 2.4. sFRP5 Regulates Adipocyte Size During Obesity in a Tissue Autonomous Manner. **A**, Male wild type (n=4) and sFRP5^{Q27stop} (n=4) mice were fed a high fat diet for six weeks. G-WAT was excised and weighed. Data are expressed as mean plus S.D. **B**, Gonadal adipose tissue was portioned into four quadrants for further analysis. **C**, Size of adipocytes in quadrants 1-4 were determined by MetaMorph analysis and plotted as percentage of large cells (> 8000 μm^2) plus S.D. **D**, The average numbers of CLS from quadrants 1-4 are presented as mean plus S.D. **E**, Gonadal adipose tissue from wild type (n=6) or sFRP5^{Q27stop} (n=6) donors was transplanted subcutaneously into *db/db* (n=3) recipients at four weeks of age. **F**, Tissue transplants were harvested after ten weeks and subjected to morphometric analysis. Data are expressed as percentage of large cells (> 8000 μm^2) plus S.D. in donor mice before and after transplantation. G-WAT, gonadal white adipose tissue; CLS, crown-like structures. Significance was determined using Student's t-test. *P*-values < 0.05 are depicted with an asterisk. *P*-values < 0.1 are marked with a cross.

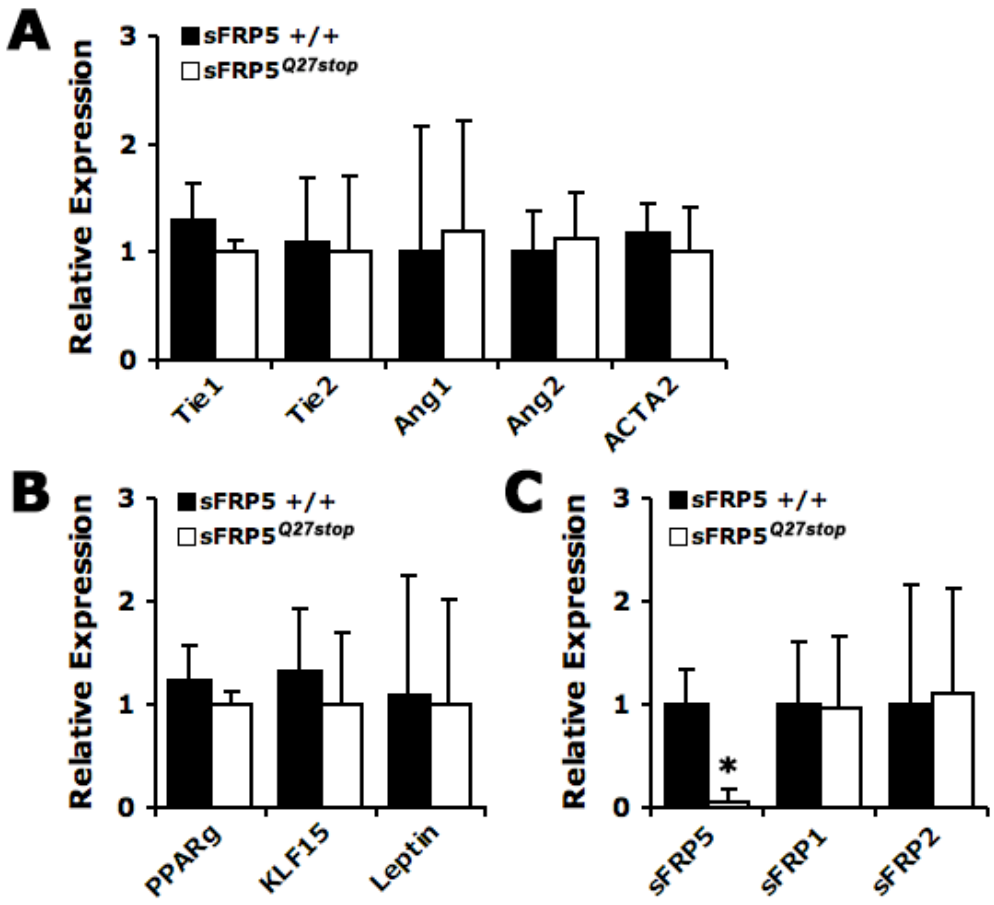

Figure 2.5. Relative Expression of Adipocyte and Vasculature Markers in sFRP5^{Q27stop} Mice. **A**,**B**,**C**, RNA was isolated from gonadal adipose tissue of female wild type and sFRP5^{Q27stop} mice that had been challenged with a high fat diet. mRNA expression of the indicated vasculature markers (A), adipocyte markers (B), and sFRP transcripts (C) was determined by qPCR. Data are expressed as mean plus S.D. Significance was determined using Student's t-test. *P*-values < 0.05 are depicted with an asterisk.

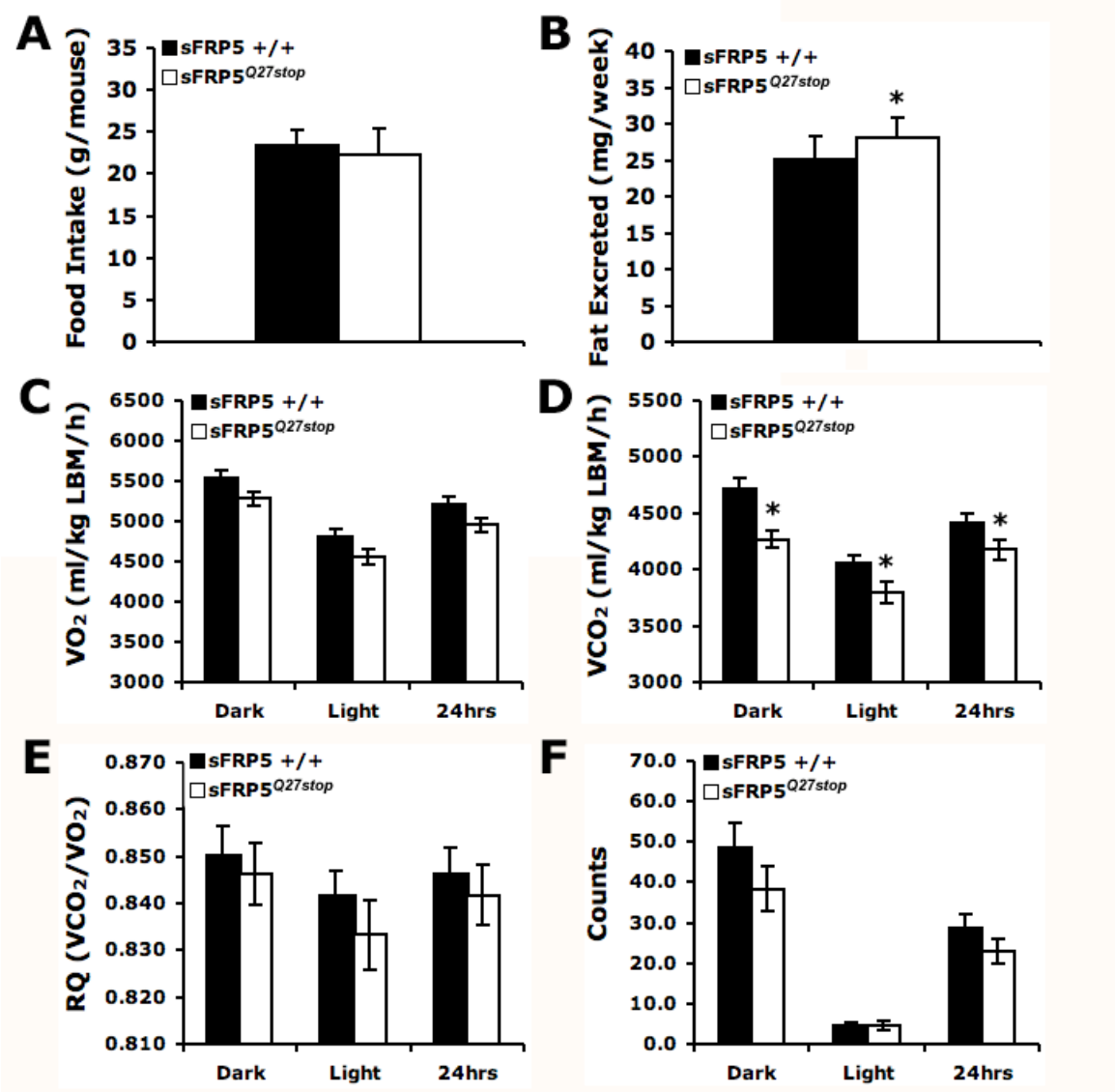

Figure 2.6. Metabolic Phenotype of Mice Harboring the sFRP5^{Q27stop} Mutation. **A**, Male wild type (n=15) and sFRP5^{Q27stop} (n=10) mice fed a high fat diet for 10 weeks were individually housed and food intake was measured every 2 days for 1 week. Data are expressed as average food consumed per animal in 1 week plus SD. **B**, Mice were housed as in A and feces was collected at the end of 1 week and subjected to fecal fat analysis. Data are expressed as average fat excreted in 1 week plus SD. **C**,**D**,**E**,**F**, Male Wild type (n=15) and sFRP5^{Q27stop} (n=13) mice were placed in a comprehensive lab animal monitoring system (CLAMS) for 3 days. Data from day 3 are expressed as mean ± SEM for (C) oxygen consumption, (D) carbon dioxide production, (E) respiratory quotient, and (F) Z-activity. Significance was determined using Student's t-test. *P*-values < 0.05 are depicted with an asterisk.

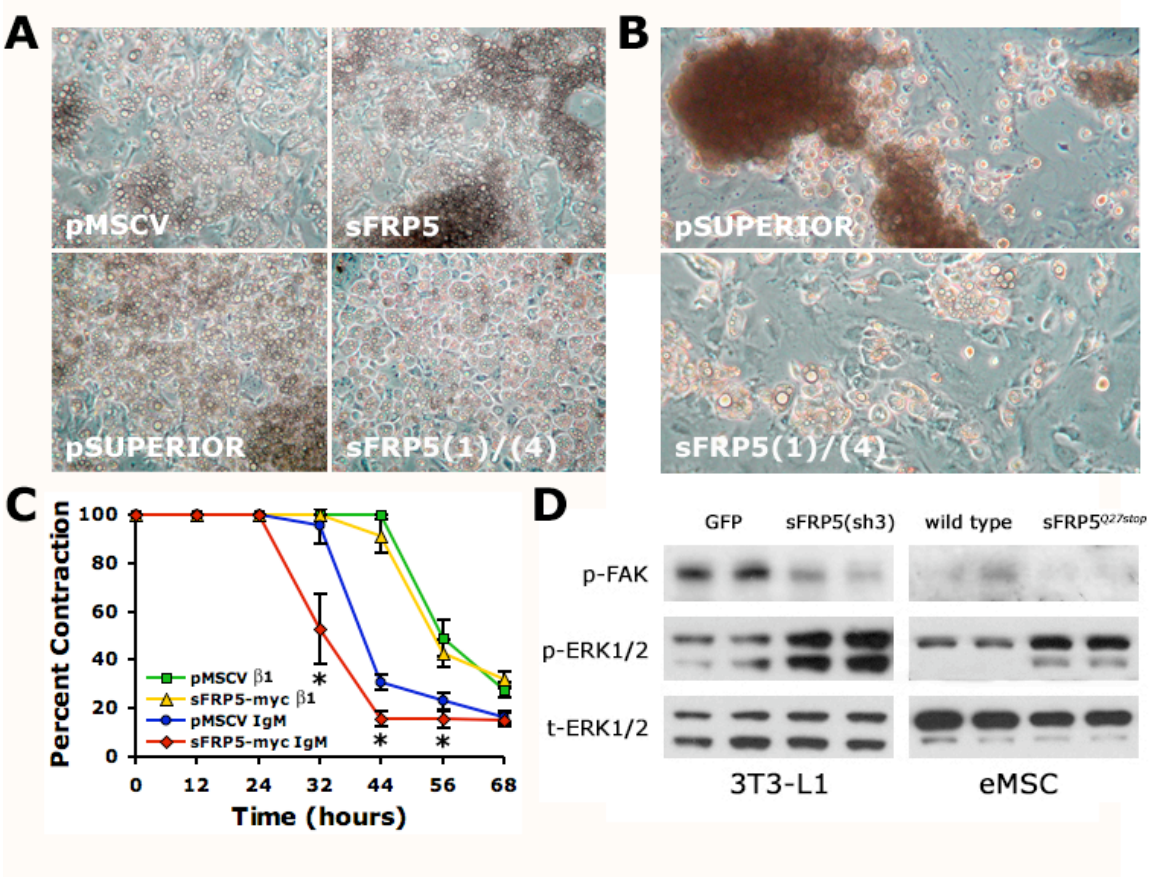

Figure 2.7. Integrin Signaling may Mediate sFRP5-Regulated Adipocyte Clustering. **A**, 3T3-L1 preadipocytes were infected with constructs expressing sFRP5 or short hairpin RNAs, (1) and (4), against sFRP5 and induced to differentiate along with vector controls in the presence of insulin and dexamethasone. Images were taken 12 days post induction. **B**, sFRP5 deficient 3T3-L1 adipocytes were released with EDTA and re-plated onto culture dishes coated with collagen type IV. Images were taken within one hour of re-plating. **C**, 3T3-L1 preadipocytes expressing sFRP5-myc were imbedded in collagen type I gels in the presence of integrin β1 blocking antibody or IgM isotype control antibody. Percent contraction of the gels was measured over time as described in materials and methods. Data are expressed as mean plus S.D. **D**, sFRP5-deficient 3T3-L1 cells or eMSCs derived from sFRP5^{Q27stop} mice were induced to differentiate as described in materials and methods. Cells were starved for four hours in DPBS then stimulated with 20 or 100 nM insulin for 30 minutes and harvested as whole cell lysates. Activation of factors downstream of integrin signaling was measured by western blot. p-FAK, phospho-focal adhesion kinase; p-ERK1/2, phospho-extracellular signal-regulated kinases 1/2; t-ERK1/2, total ERK1/2. Significance was determined using Student's t-test. *P*-values < 0.05 are depicted with an asterisk.

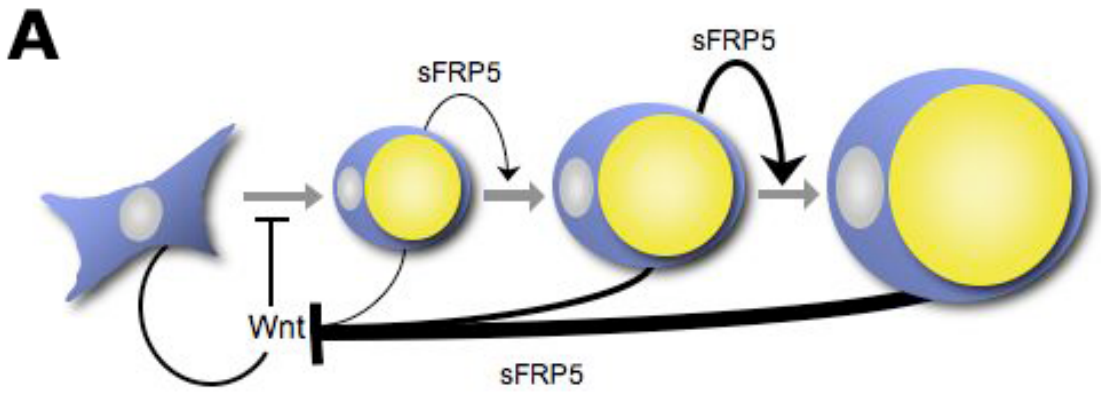

Figure 2.8. sFRP5 Regulates Adipocyte Growth and Preadipocyte Recruitment. In this model, expanding adipocytes secrete higher levels of sFRP5, which further influences adipocyte growth during obesity. Additionally, sFRP5 may feedback to inhibit autocrine Wnt signaling in preadipocytes, thus allowing the recruitment and differentiation of new adipocytes to facilitate increased lipid accumulation.

References

1. Logan CY, Nusse R: **The Wnt signaling pathway in development and disease**. *Annu Rev Cell Dev Biol* 2004, **20**:781-810.

2. Clevers H: **Wnt/beta-catenin signaling in development and disease**. *Cell* 2006, **127**:469-480.

3. Jones SE, Jomary C: **Secreted Frizzled-related proteins: searching for relationships and patterns**. *Bioessays* 2002, **24**:811-820.

4. Melkonyan HS, Chang WC, Shapiro JP, Mahadevappa M, Fitzpatrick PA, Kiefer MC, Tomei LD, Umansky SR: **SARPs: a family of secreted apoptosis-related proteins**. *Proc Natl Acad Sci U S A* 1997, **94**:13636-13641.

5. Finch PW, He X, Kelley MJ, Uren A, Schaudies RP, Popescu NC, Rudikoff S, Aaronson SA, Varmus HE, Rubin JS: **Purification and molecular cloning of a secreted, Frizzled-related antagonist of Wnt action**. *Proc Natl Acad Sci U S A* 1997, **94**:6770-6775.

6. Bafico A, Gazit A, Pramila T, Finch PW, Yaniv A, Aaronson SA: **Interaction of frizzled related protein (FRP) with Wnt ligands and the frizzled receptor suggests alternative mechanisms for FRP inhibition of Wnt signaling**. *J Biol Chem* 1999, **274**:16180-16187.

7. Uren A, Reichsman F, Anest V, Taylor WG, Muraiso K, Bottaro DP, Cumberledge S, Rubin JS: **Secreted frizzled-related protein-1 binds directly to Wingless and is a biphasic modulator of Wnt signaling**. *J Biol Chem* 2000, **275**:4374-4382.

8. Satoh W, Matsuyama M, Takemura H, Aizawa S, Shimono A: **Sfrp1, Sfrp2, and Sfrp5 regulate the Wnt/beta-catenin and the planar cell polarity pathways during early trunk formation in mouse**. *Genesis* 2008, **46**:92-103.

9. Bhat RA, Stauffer B, Komm BS, Bodine PV: **Structure-function analysis of secreted frizzled-related protein-1 for its Wnt antagonist function**. *J Cell Biochem* 2007, **102**:1519-1528.

10. Galli LM, Barnes T, Cheng T, Acosta L, Anglade A, Willert K, Nusse R, Burrus LW: **Differential inhibition of Wnt-3a by Sfrp-1, Sfrp-2, and Sfrp-3**. *Dev Dyn* 2006, **235**:spc1.

11. Yoshino K, Rubin JS, Higinbotham KG, Uren A, Anest V, Plisov SY, Perantoni AO: **Secreted Frizzled-related proteins can regulate metanephric development**. *Mech Dev* 2001, **102**:45-55.

12. Suzuki H, Watkins DN, Jair KW, Schuebel KE, Markowitz SD, Chen WD, Pretlow TP, Yang B, Akiyama Y, Van Engeland M, et al.: **Epigenetic inactivation of SFRP genes allows constitutive WNT signaling in colorectal cancer**. *Nat Genet* 2004, **36**:417-422.

13. Nojima M, Suzuki H, Toyota M, Watanabe Y, Maruyama R, Sasaki S, Sasaki Y, Mita H, Nishikawa N, Yamaguchi K, et al.: **Frequent epigenetic inactivation of SFRP genes and constitutive activation of Wnt signaling in gastric cancer**. *Oncogene* 2007, **26**:4699-4713.

14. Fukui T, Kondo M, Ito G, Maeda O, Sato N, Yoshioka H, Yokoi K, Ueda Y, Shimokata K, Sekido Y: **Transcriptional silencing of secreted frizzled related protein 1 (SFRP 1) by promoter hypermethylation in non-small-cell lung cancer**. *Oncogene* 2005, **24**:6323-6327.

15. Elston MS, Gill AJ, Conaglen JV, Clarkson A, Shaw JM, Law AJ, Cook RJ, Little NS, Clifton-Bligh RJ, Robinson BG, et al.: **Wnt pathway inhibitors are strongly down-regulated in pituitary tumors**. *Endocrinology* 2008, **149**:1235-1242.

16. Liu TH, Raval A, Chen SS, Matkovic JJ, Byrd JC, Plass C: **CpG island methylation and expression of the secreted frizzled-related protein gene family in chronic lymphocytic leukemia**. *Cancer Res* 2006, **66**:653-658.

17. Fodde R, Smits R, Clevers H: **APC, signal transduction and genetic instability in colorectal cancer**. *Nat Rev Cancer* 2001, **1**:55-67.

18. Bovolenta P, Esteve P, Ruiz JM, Cisneros E, Lopez-Rios J: **Beyond Wnt inhibition: new functions of secreted Frizzled-related proteins in development and disease**. *J Cell Sci* 2008, **121**:737-746.

19. Rodriguez J, Esteve P, Weinl C, Ruiz JM, Fermin Y, Trousse F, Dwivedy A, Holt C, Bovolenta P: **SFRP1 regulates the growth of retinal ganglion cell axons through the Fz2 receptor**. *Nat Neurosci* 2005, **8**:1301-1309.

20. Dufourcq P, Leroux L, Ezan J, Descamps B, Lamaziere JM, Costet P, Basoni C, Moreau C, Deutsch U, Couffinhal T, et al.: **Regulation of endothelial cell cytoskeletal reorganization by a secreted frizzled-related protein-1 and frizzled 4- and frizzled 7-dependent pathway: role in neovessel formation**. *Am J Pathol* 2008, **172**:37-49.

21. Lee JL, Lin CT, Chueh LL, Chang CJ: **Autocrine/paracrine secreted Frizzled-related protein 2 induces cellular resistance to apoptosis: a possible mechanism of mammary tumorigenesis**. *J Biol Chem* 2004, **279**:14602-14609.

22. Hausler KD, Horwood NJ, Chuman Y, Fisher JL, Ellis J, Martin TJ, Rubin JS, Gillespie MT: **Secreted frizzled-related protein-1 inhibits RANKL-dependent osteoclast formation**. *J Bone Miner Res* 2004, **19**:1873-1881.

23. Lee HX, Ambrosio AL, Reversade B, De Robertis EM: **Embryonic dorsal-ventral signaling: secreted frizzled-related proteins as inhibitors of tolloid proteinases**. *Cell* 2006, **124**:147-159.

24. Muraoka O, Shimizu T, Yabe T, Nojima H, Bae YK, Hashimoto H, Hibi M: **Sizzled controls dorso-ventral polarity by repressing cleavage of the Chordin protein**. *Nat Cell Biol* 2006, **8**:329-338.

25. Koza RA, Nikonova L, Hogan J, Rim JS, Mendoza T, Faulk C, Skaf J, Kozak LP: **Changes in gene expression foreshadow diet-induced obesity in genetically identical mice**. *PLoS Genet* 2006, **2**:e81.

26. Gerin I, Dolinsky VW, Shackman JG, Kennedy RT, Chiang SH, Burant CF, Steffensen KR, Gustafsson JA, MacDougald OA: **LXRbeta is required for adipocyte growth, glucose homeostasis, and beta cell function**. *J Biol Chem* 2005, **280**:23024-23031.

27. Quwailid MM, Hugill A, Dear N, Vizor L, Wells S, Horner E, Fuller S, Weedon J, McMath H, Woodman P, et al.: **A gene-driven ENU-based approach to generating an allelic series in any gene**. *Mamm Genome* 2004, **15**:585-591.

28. Student AK, Hsu RY, Lane MD: **Induction of fatty acid synthetase synthesis in differentiating 3T3-L1 preadipocytes**. *J Biol Chem* 1980, **255**:4745-4750.

29. Hemati N, Ross SE, Erickson RL, Groblewski GE, MacDougald OA: **Signaling pathways through which insulin regulates CCAAT/enhancer binding protein alpha (C/EBPalpha) phosphorylation and gene expression in 3T3-L1 adipocytes. Correlation with GLUT4 gene expression**. *J Biol Chem* 1997, **272**:25913-25919.

30. Rim JS, Mynatt RL, Gawronska-Kozak B: **Mesenchymal stem cells from the outer ear: a novel adult stem cell model system for the study of adipogenesis**. *Faseb J* 2005, **19**:1205-1207.

31. Keller P, Petrie JT, De Rose P, Gerin I, Wright WS, Chiang SH, Nielsen AR, Fischer CP, Pedersen BK, Macdougald OA: **Fat-specific Protein 27 Regulates Storage of Triacylglycerol**. *J Biol Chem* 2008, **283**:14355-14365.

32. Ross SE, Hemati N, Longo KA, Bennett CN, Lucas PC, Erickson RL, MacDougald OA: **Inhibition of adipogenesis by Wnt signaling**. *Science* 2000, **289**:950-953.

33. Rodbell M: **Metabolism of Isolated Fat Cells. I. Effects of Hormones on Glucose Metabolism and Lipolysis**. *J Biol Chem* 1964, **239**:375-380.

34. Wright WS, Longo KA, Dolinsky VW, Gerin I, Kang S, Bennett CN, Chiang SH, Prestwich TC, Gress C, Burant CF, et al.: **Wnt10b inhibits obesity in ob/ob and agouti mice**. *Diabetes* 2007, **56**:295-303.

35. Folch J, Lees M, Sloane Stanley GH: **A simple method for the isolation and purification of total lipides from animal tissues**. *J Biol Chem* 1957, **226**:497-509.

36. Murano I, Barbatelli G, Parisani V, Latini C, Muzzonigro G, Castellucci M, Cinti S: **Dead adipocytes, detected as crown-like structures (CLS), are prevalent in visceral fat depots of genetically obese mice**. *J Lipid Res* 2008.

37. Cao Y: **Angiogenesis modulates adipogenesis and obesity**. *J Clin Invest* 2007, **117**:2362-2368.

38. Dallabrida SM, Zurakowski D, Shih SC, Smith LE, Folkman J, Moulton KS, Rupnick MA: **Adipose tissue growth and regression are regulated by angiopoietin-1**. *Biochem Biophys Res Commun* 2003, **311**:563-571.

39. Calderwood DA: **Integrin activation**. *J Cell Sci* 2004, **117**:657-666.

40. Liu J, DeYoung SM, Zhang M, Zhang M, Cheng A, Saltiel AR: **Changes in integrin expression during adipocyte differentiation**. *Cell Metab* 2005, **2**:165-177.

41. Schiro JA, Chan BM, Roswit WT, Kassner PD, Pentland AP, Hemler ME, Eisen AZ, Kupper TS: **Integrin alpha 2 beta 1 (VLA-2) mediates reorganization and contraction of collagen matrices by human cells**. *Cell* 1991, **67**:403-410.

42. Cooke ME, Sakai T, Mosher DF: **Contraction of collagen matrices mediated by alpha2beta1A and alpha(v)beta3 integrins**. *J Cell Sci* 2000, **113 (Pt 13)**:2375-2383.

43. Farnier C, Krief S, Blache M, Diot-Dupuy F, Mory G, Ferre P, Bazin R: **Adipocyte functions are modulated by cell size change: potential involvement of an integrin/ERK signalling pathway**. *Int J Obes Relat Metab Disord* 2003, **27**:1178-1186.

44. Xu Q, Wang Y, Dabdoub A, Smallwood PM, Williams J, Woods C, Kelley MW, Jiang L, Tasman W, Zhang K, et al.: **Vascular development in the retina and inner ear: control by Norrin and Frizzled-4, a high-affinity ligand-receptor pair**. *Cell* 2004, **116**:883-895.

45. Zerlin M, Julius MA, Kitajewski J: **Wnt/Frizzled signaling in angiogenesis**. *Angiogenesis* 2008, **11**:63-69.

46. Chun TH, Hotary KB, Sabeh F, Saltiel AR, Allen ED, Weiss SJ: **A pericellular collagenase directs the 3-dimensional development of white adipose tissue**. *Cell* 2006, **125**:577-591.

47. Banyai L, Patthy L: **The NTR module: domains of netrins, secreted frizzled related proteins, and type I procollagen C-proteinase enhancer protein are homologous with tissue inhibitors of metalloproteases**. *Protein Sci* 1999, **8**:1636-1642.

48. Henegar C, Tordjman J, Achard V, Lacasa D, Cremer I, Guerre-Millo M, Poitou C, Basdevant A, Stich V, Viguerie N, et al.: **Adipose tissue transcriptomic signature highlights the pathological relevance of extracellular matrix in human obesity**. *Genome Biol* 2008, **9**:R14.

Chapter III

Expanding the Scope of sFRP5 Function

Introduction

sFRPs comprise a class of endogenous inhibitors of Wnt signaling that are expressed in many tissues throughout development and adulthood [1]. A growing literature is now uncovering the functions of many sFRPs in biological and pathological processes [2]; however, a specific role for sFRP5 has not been as forthcoming. In the previous chapter we presented data demonstrating a novel function for sFRP5 in adipocyte biology and obesity. In the current chapter we describe additional preliminary results suggesting that sFRP5 may directly or indirectly regulate the seemingly distinct processes governing food intake under specific conditions, bone mass, and local metabolism in adipocytes.

Utilizing high fat-challenged sFRP5^{Q27stop} mice we show that food intake, while not different under standard room temperature conditions, is decreased compared to wild type mice when animals are housed at 27^{o}C, a temperature approaching the thermoneutral zone in mice. This occurs with no detectable difference in total body weight between wild type and sFRP5^{Q27stop} mice.

Stemming from numerous recent reports suggesting a primary role for Wnt signaling in the regulation of bone mass [3-7], we performed microcomputerized tomography (μCT) analysis on femurs from wild type and sFRP5^{Q27stop} mice.

Interestingly, our analysis revealed a decrease in cortical bone mineral density and content in mice lacking functional sFRP5.

To gain a global perspective of genes or pathways that may be regulated by sFRP5, we performed a microarray analysis on RNA isolated from G-WAT of high fat-fed wild type and sFRP5^{Q27stop} mice. Results from this experiment suggest that there may be an upregulation of genes involved in mitochondrial oxidative phosphorylation in sFRP5^{Q27stop} mice, hinting at possible alterations of adipocyte metabolism in these animals.

Thus, in the current chapter we describe various pieces of data that may expand the scope of sFRP5 function and provide additional insight into the overall impact of this factor on vertebrate biology.

Materials and Methods

Animals

Animal care was overseen by the Unit for Laboratory Animal Medicine (University of Michigan). sFRP5^{Q27stop} mice were generated by ENU mutagenesis in which a C79T mutation created a premature stop codon at Gln 27, likely producing a null allele [8]. All animals were individually housed as indicated at room temperature or in a controlled temperature room set at 27^{o}C with a regular 12-hour light/dark cycle and were fed *ad libitum* with a high fat diet (4.73 kcal/g, 45% fat, D12451, Research Diets) for 12-18 weeks.

Fasted Blood Glucose and Serum Insulin

Mice were fasted for 12 hours prior to experimentation. Blood glucose was measured in wild type and sFRP5^{Q27stop} tail blood with the OneTouch UltraTM glucometer (Lifescan, Burnaby, British Columbia, Canada). Serum insulin was determined using an enzyme-linked immunosorbent assay kit (Crystal Chem, Downers Grove, IL) according to the manufacturer's instructions.

Microcomputerized Tomography (μCT)

μCT was used to analyze femurs from hindlimbs of female wild type and sFRP5^{Q27stop} mice challenged with a high fat diet as described [9] by using the Stereology function of GE Medical Systems MICROVIEW software.

Microarray Analysis

RNA was isolated from G-WAT of male wild type and sFRP5^{Q27stop} mice. cDNA was amplified and purified using the WT Pico assay (NuGen Inc.) following the manufacturer's standard protocol. Four micrograms of cDNA was converted to sense orientation using the Exon Module (NuGen Inc.) and subsequently fragmented and biotinylated using the Ovation FL Module (NuGen Inc.) following the manufacturers standard protocol. The probe was then hybridized to Affymetrix Mouse Gene ST 1.0 GeneChips for 20 hours at 45^{o}C, stained, and washed using a Fluidics FS450 instrument, and then scanned with the Affymetrix 7G Scanner 3000. Data were analyzed using Ingenuity Pathway Analysis software (Ingenuity Systems, Redwood City, CA) to identify relevant biological networks.

Results

Temperature Dependent Effects on Food Intake in sFRP5^{Q27stop} Mice

To define further the conditions of obesity resistance in sFRP5^{Q27stop} mice, we challenged both male and female wild type and sFRP5^{Q27stop} mice at four weeks of age with a high fat diet, measuring total body weight and food intake at regular intervals over a 12-week period. Mice were individually housed at room temperature (25^{o}C) for the first six weeks (weeks 1-6) and at 27^{o}C for the last six weeks (weeks 7-12). This design allowed us to test whether environmental factors play a role in obesity resistance in this model, and whether slight differences in food intake over time may contribute to decreases in body weight and fat mass in male or female sFRP5^{Q27stop} mice. Somewhat unexpectedly based on our previous data, no differences in total body weight were observed between male or female wild type and sFRP5^{Q27stop} mice over the 12-week period (Figure 3.1a, and data not shown). Despite this observation, food intake was decreased in female sFRP5^{Q27stop} mice housed at 27^{o}C (weeks 7-12), while there was no change in food intake when these mice were housed at room temperature (weeks 1-6) (figure 3.1b).

The finding that food intake was altered without concomitant changes in body weight led us to question whether there were differences in body composition that were not reflected in the total body weight. However, our analysis of G-WAT and dorsolumbar white adipose tissue (D-WAT) revealed no

difference in the weight of these adipose depots between wild type and sFRP5^{Q27stop} mice (Figure 3.1c).

To determine whether insulin or glucose homeostasis was affected under these conditions, wild type and sFRP5^{Q27stop} mice were fasted for 12 hours at the conclusion of the experiment (week 12) and analyzed for blood glucose and serum insulin levels. Our results indicate that there are no differences in fasted blood glucose or fasted serum insulin in high fat-fed wild type and sFRP5^{Q27stop} mice housed at 27^{o}C (Figure 3.1d).

Taken together, our results suggest that under certain environmental conditions, food intake is decreased in sFRP5^{Q27stop} mice compared to controls, and that this occurs without an attendant decrease in total body weight or alteration of glucose and insulin homeostasis.

μCT Analysis of Cortical and Trabecular Bone in sFRP5^{Q27stop} Mice

Numerous recent reports have confirmed that several Wnt pathway members, including sFRPs, play a central role in the regulation of bone mass in mammals [3-7]. As deletion of sFRP1 leads to increased trabecular bone formation [5] and targeted overexpression of sFRP4 promotes a low bone mass phenotype [6], we sought to characterize the effect of sFRP5 on bone mass in sFRP5^{Q27stop} mice. Wild type and sFRP5^{Q27stop} mice were challenged with a high fat diet for 18 weeks, following which femurs were collected and submitted for μCT analysis of cortical and trabecular bone. Our results suggest that bone

mineral density (BMD), bone mineral content (BMC), and the outer perimeter of cortical bone are decreased in sFRP5^{Q27stop} femurs (Figure 3.2a,b,c).

Since Wnt signaling has been shown to play a particularly important role in trabecular bone formation, we hypothesized that sFRP5 may affect this process. However, μCT analysis of trabecular bone formation in sFRP5^{Q27stop} mice revealed no difference in BMD, BMC, or bone volume fraction (Figure 3.2d,e,f) in femurs from sFRP5^{Q27stop} mice compared to wild type controls.

Investigation of mRNA isolated by flushing the marrow cavity of C57BL/6J femurs suggests that sFRP5 is not expressed in bone marrow (data not shown). Thus, while our data suggest that sFRP5 regulates cortical bone formation, it is possible that this may be an indirect effect.

Microarray Analysis of G-WAT from sFRP5^{Q27stop} mice

To obtain a global perspective of genes or cellular pathways that may be regulated by sFRP5, we performed a microarray analysis on G-WAT from male high-fat-challenged wild type and sFRP5^{Q27stop} mice. This cohort was the male counterpart to the female cohort described in figure 3.1. As described above, the mice were challenged with a high fat diet at four weeks of age for 12 weeks. Like the female cohort reported in figure 3.1, male mice did not exhibit a difference in total body weight (data not shown). In contrast to findings with female mice, however, male wild type and sFRP5^{Q27stop} mice did not show a difference in food intake (data not shown). Therefore, this cohort was selected for subsequent microarray analysis based on the above observations, enabling us to evaluate

changes in gene expression resulting from loss of sFRP5 and not general differences associated with altered body weight or food intake.

Microarray data were analyzed using Ingenuity Pathway Analysis (IPA) software to identify relevant biological networks or pathways that may be altered in sFRP5^{Q27stop} mice compared to wild type controls. Approximately 3,000 probe sets were populated into the IPA program and about 850 were eligible for network/pathways analysis. Table 3.1 shows the top 10 pathways identified by IPA of differentially expressed genes. The pathways identified as Oxidative Phosphorylation and Mitochondrial Dysfunction are highly regulated and contain a number of genes involved in oxidative phosphorylation that are statistically upregulated in adipose tissue from sFRP5^{Q27stop} mice (Table 3.1).

Networks generated from IPA reveal an upregulation of cytochrome c oxidase subunits Cox7b, Cox17, Cox6b1, Cox6a1, Cox6c, Cox5b, Cox2, and Cox7c (Figure 3.3). Interestingly, our microarray data also indicate that the Huntingtin protein (HTT) is downregulated in sFRP5^{Q27stop} adipose tissue. HTT has been suggested to regulate cellular energetics, in part through alterations in the activity of complex II in the electron transport chain [10]. In addition to cytochrome c oxidase (complex IV) subunits, ATP synthase subunits Atp6vd1, Atp5l, Atp5g2, Atp5h, Atp6v1g1, and Atp6v1g2 are increased in sFRP5^{Q27stop} adipose tissue, as are NADH2 dehydrogenase subcomplexes, Ndufb5, Ndufa1, Ndufa13, Ndufa6, Ndufb6, and Ndufs6 (Figure 3.4). Moreover, Gene Ontology (GO) analysis found that oxidative phosphorylation was one of the biological processes over-represented in adipose tissue from sFRP5^{Q27stop} mice (data not

shown). Thus, the results of our microarray analyses support the hypothesis that oxidative phosphorylation is increased in adipocytes of sFRP5^{Q27stop} mice.

Discussion

Here we provide evidence that sFRP5 may influence food intake under certain conditions. Our data also suggest that sFRP5 regulates cortical bone mass and possibly oxidative phosphorylation in adipocytes. While these effects are somewhat diverse with regard to mechanism, the results serve to highlight a broader scope for sFRP5 function in vertebrate biology.

The finding that food intake is decreased in sFRP5^{Q27stop} mice is interesting as this effect was only observed once the mice were housed at 27^{o}C. This implies that there may be interactions between sFRP5 function and environmental factors, such as temperature. Alternatively, it could be argued that food intake appeared to be decreasing in sFRP5^{Q27stop} mice prior to the animals being housed at 27^{o}C, and that if left at room temperature, the differences may have reached statistical significance. In any case, it is tempting to extrapolate the data and speculate that decreases in food intake over time are the cause of obesity resistance in sFRP5^{Q27stop} mice (Figure 2.3). However, it is important to remember that we observed a decrease in fat mass and total body weight in sFRP5^{Q27stop} mice under entirely different experimental conditions than those outlined in the current chapter. For example, in the experiments performed previously, wild type and sFRP5^{Q27stop} mice were placed on a high fat diet beginning at 12-16 weeks of age, while the cohort described in the current

chapter began receiving the same diet at four weeks of age. Also, the mice described here were housed at two different temperatures, while the mice described in chapter II were kept at a constant temperature (room temperature) throughout the entire experiment. Furthermore, our previous data from the adipose tissue transplantation implies that differences in adipocyte growth during obesity are not dependent on food intake. Therefore, pending further experimentation, we cannot conclude that the previously reported decrease in fat mass and body weight observed in sFRP5^{Q27stop} mice is a result of decreased food intake.

Additionally, while our finding that fasted plasma insulin is similar in wild type and sFRP5^{Q27stop} mice may seem at odds with previous observations in chapter II, it should be noted that insulin was measured here during a fasted state, while the previous data was obtained during the fed state. Nonetheless, the fact that fasted insulin levels are similar in the same cohort that show no statistical difference in body weight suggests that the differences in fed insulin levels observed in chapter II may simply be a reflection of altered adiposity in sFRP5^{Q27stop} mice, and not a direct effect on insulin secretion *per se*.

As Wnt signaling has recently been shown to regulate multiple aspects of bone biology, we sought to determine whether sFRP5^{Q27stop} mice exhibit a bone phenotype. Here we show that cortical bone parameters, BMD, BMC, and outer perimeter, are all decreased in sFRP5^{Q27stop} mice as measured by μCT. This was somewhat unexpected based on the established role of Wnt signaling in bone formation. We reasoned that if sFRP5 were acting as a classical Wnt

inhibitor in this context, then we would expect to observe an increase in bone formation in sFRP5^{Q27stop} mice, where presumably Wnt activity is high. However, we observed the opposite result in cortical bone and no effect on trabecular bone. Our attempts to quantify sFRP5 mRNA expression in bone marrow led us to conclude that sFRP5 is not expressed, or is expressed at very low levels, in that tissue. Therefore, we speculate that the effect seen in cortical bone of sFRP5^{Q27stop} mice is likely an indirect effect, possibly due to the altered adiposity we observed previously.

Our attempt to identify genes or pathways altered in sFRP5^{Q27stop} mice led to the finding that oxidative phosphorylation may be increased in these animals. Microarray analysis revealed an increase in expression of genes whose products comprise many of the proteins involved in complexes I, IV, and V of the electron transport chain. Specifically, subunits of cytochrome c oxidase, NADH2 dehydrogenase, and ATP synthase were all upregulated in sFRP5^{Q27stop} adipose tissue compared to controls.

In light of previous observations that sFRP5^{Q27stop} mice exhibit a smaller proportion of large adipocytes in the obese state, the finding that oxidative phosphorylation may be increased in sFRP5^{Q27stop} mice supports a hypothesis wherein increased oxidation of fatty acids may underlie differences in adipocyte size. Although no differences were observed in whole body oxygen consumption of sFRP5^{Q27stop} mice (Figure 2.6c), undetected changes in local adipocyte metabolism may contribute to small but significant differences in adipocyte volume over time.

To test this hypothesis, mitochondrial size and number should be evaluated in wild type and sFRP5^{Q27stop} adipocytes to determine whether mitochondrial biogenesis is altered. Furthermore, β-oxidation and oxygen consumption should be measured in adipocytes from sFRP5^{Q27stop} mice to investigate possible alterations in local metabolism that may underlie the observations previously reported (Figure 2.3, 2.4).

Here we have provided additional preliminary data suggesting a role for sFRP5 in the regulation of bone mass, adipocyte metabolism, and food intake under certain conditions. Though seemingly unrelated, these effects are not entirely unexpected as sFRP5 function is disrupted in all tissues of sFRP5^{Q27stop} mice. Thus, our data strengthen the notion that sFRP5 plays diverse roles in regulating multiple aspects of vertebrate biology during obesity.

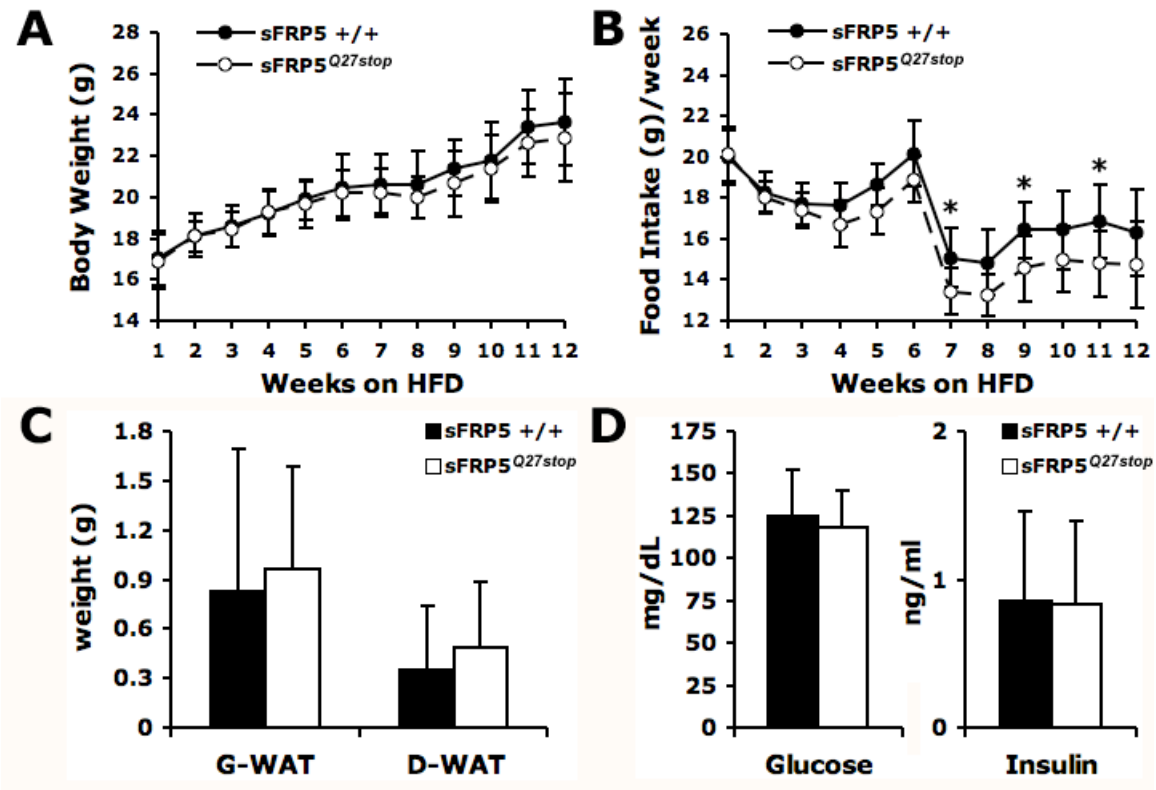

Figure 3.1. Temperature Dependent Effects on Food Intake in sFRP5^{Q27stop} Mice. **A**, Four week old female wild type (n=8) and sFRP5^{Q27stop} (n=10) mice were challenged with a high fat diet for 12 weeks while housed at either room temperature (weeks 1-6) or at 27^{o}C (weeks 7-12). Total body weight was measured every week. Data are expressed as mean ± S.D. **B**, Food intake was measured once (weeks 1-6) or twice (weeks 7-12) a week for 12 weeks. Data are expressed as mean food intake per week ± S.D. **C**, G-WAT and D-WAT were excised and weighed. Data are expressed as mean plus S.D. **D**, Fasted blood glucose and serum insulin were measured at the end of the 12-week period. Data are expressed as mean plus S.D. HFD, high fat diet. G-WAT, gonadal white adipose tissue; D-WAT, dorsolumbar white adipose tissue. Significance was determined using Student's t-test. *P*-values < 0.05 are depicted with an asterisk.

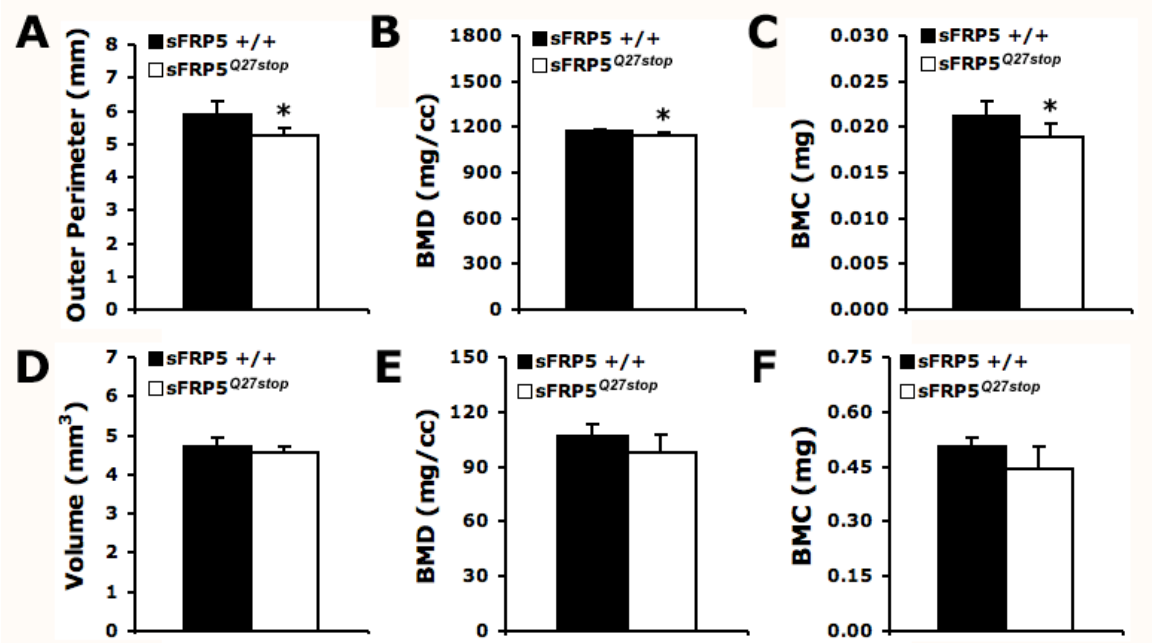

Figure 3.2. μCT Analysis of Cortical and Trabecular Bone in sFRP5^{Q27stop} Mice. **A**,**B**,**C**, μCT analysis conducted on cortical bone from femurs of female wild type (n=5) and sFRP5^{Q27stop} (n=6) mice measured (A) outer perimeter, (B) BMD, and (C) BMC. **D**,**E**,**F**, μCT analysis conducted on trabecular bone from the same femurs measured (D) volume, (E) BMD, and (F) BMC. Data are expressed as mean plus S.D. μCT, microcomputerized tomography; BMD, bone mineral density; BMC, bone mineral content. Significance was determined using Student's t-test. *P*-values < 0.05 are depicted with an asterisk.

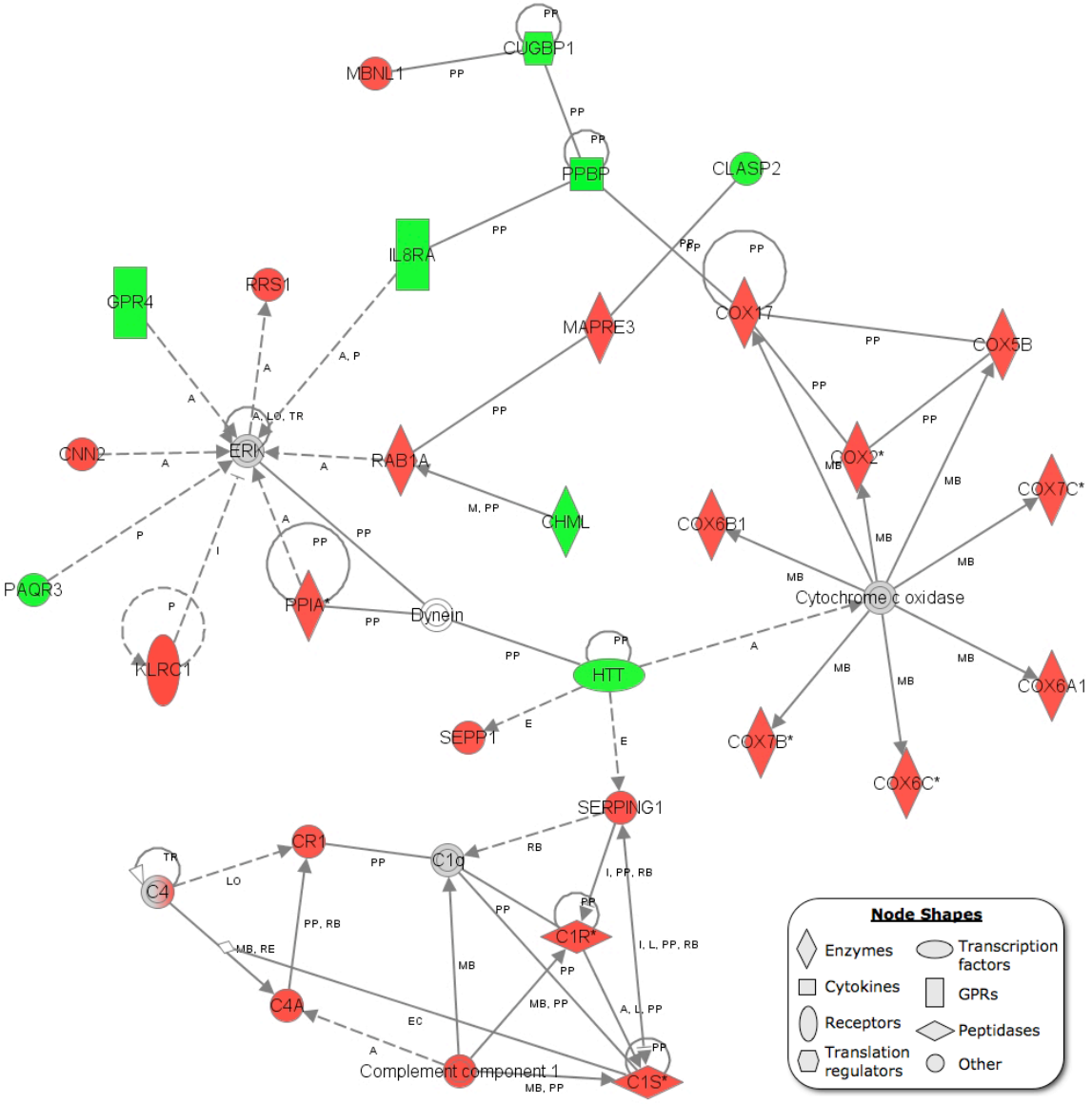

Figure 3.3. Ingenuity Pathway Analysis of Cytochrome C Oxidase Subunit Upregulation in sFRP5^{Q27stop} mice. Ingenuity pathway analysis of networks altered in sFRP5^{Q27stop} mice revealed an upregulation of cytochrome c oxidase subunits, seen on the right-hand side of the figure. An upregulation in complement factors is seen at the bottom of the figure. Red indicates genes that are upregulated; green indicates genes that are downregulated.

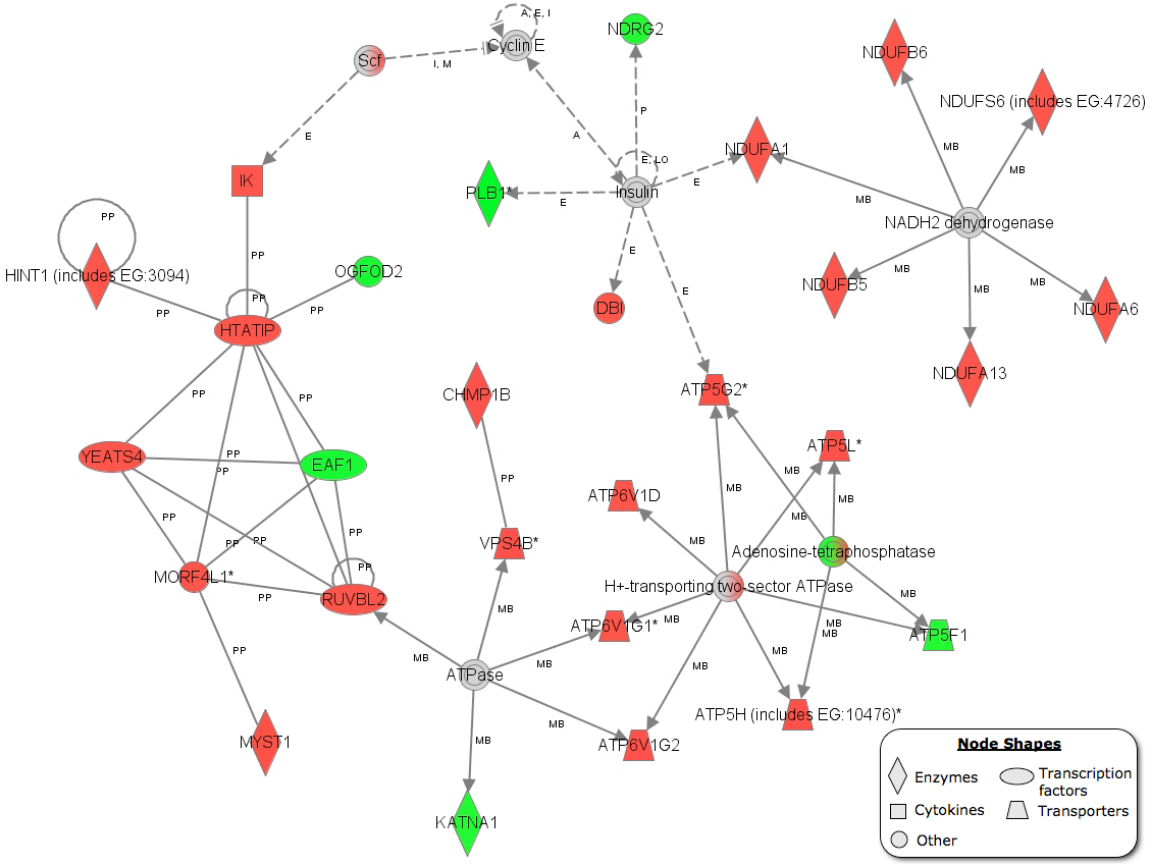

Figure 3.4. Ingenuity Pathway Analysis of NADH2 Dehydrogenase and ATP synthase Subunit Upregulation in sFRP5^{Q27stop} Mice. Ingenuity pathway analysis of networks altered in sFRP5^{Q27stop} mice revealed an upregulation of NADH2 subunits and ATP synthase subunits, seen on the upper right-hand side and lower right-hand side of the figure, respectively. Red indicates genes that are upregulated; green indicates genes that are downregulated.

Pathway	-Log(P-value)
Oxidative Phosphorylation	3.9000
Protein Ubiquitination Pathway	2.5000
Interferon Signaling	2.3300
Mitochondrial Dysfunction	1.6300
Complement System	1.5600
Hypoxia Signaling in the Cardiovascular System	1.3500
Antigen Presentation Pathway	1.2400
One Carbon Pool by Folate	1.2400
Glycine, Serine and Threonine Metabolism	1.1800
EGF Signaling	1.1700

Table 3.1. Top 10 Pathways Identified by IPA of Differentially Expressed Genes. Pathway analysis of differentially expressed genes identified by microarray analysis of adipose tissue from wild type and sFRP5^{Q27stop} mice. The pathways identified as Oxidative Phosphorylation and Mitochondrial Dysfunction are highly related and contain a number of statistically upregulated genes involved in oxidative phosphorylation.

References

1. Jones SE, Jomary C: **Secreted Frizzled-related proteins: searching for relationships and patterns**. *Bioessays* 2002, **24**:811-820.

2. Bovolenta P, Esteve P, Ruiz JM, Cisneros E, Lopez-Rios J: **Beyond Wnt inhibition: new functions of secreted Frizzled-related proteins in development and disease**. *J Cell Sci* 2008, **121**:737-746.

3. Bennett CN, Longo KA, Wright WS, Suva LJ, Lane TF, Hankenson KD, MacDougald OA: **Regulation of osteoblastogenesis and bone mass by Wnt10b**. *Proc Natl Acad Sci U S A* 2005, **102**:3324-3329.

4. Balemans W, Van Hul W: **The genetics of low-density lipoprotein receptor-related protein 5 in bone: a story of extremes**. *Endocrinology* 2007, **148**:2622-2629.

5. Bodine PV, Zhao W, Kharode YP, Bex FJ, Lambert AJ, Goad MB, Gaur T, Stein GS, Lian JB, Komm BS: **The Wnt antagonist secreted frizzled-related protein-1 is a negative regulator of trabecular bone formation in adult mice**. *Mol Endocrinol* 2004, **18**:1222-1237.

6. Nakanishi R, Akiyama H, Kimura H, Otsuki B, Shimizu M, Tsuboyama T, Nakamura T: **Osteoblast-targeted expression of Sfrp4 in mice results in low bone mass**. *J Bone Miner Res* 2008, **23**:271-277.

7. Morvan F, Boulukos K, Clement-Lacroix P, Roman Roman S, Suc-Royer I, Vayssiere B, Ammann P, Martin P, Pinho S, Pognonec P, et al.: **Deletion of a single allele of the Dkk1 gene leads to an increase in bone formation and bone mass**. *J Bone Miner Res* 2006, **21**:934-945.

8. Quwailid MM, Hugill A, Dear N, Vizor L, Wells S, Horner E, Fuller S, Weedon J, McMath H, Woodman P, et al.: **A gene-driven ENU-based approach to generating an allelic series in any gene**. *Mamm Genome* 2004, **15**:585-591.

9. Hankenson KD, Bain SD, Kyriakides TR, Smith EA, Goldstein SA, Bornstein P: **Increased marrow-derived osteoprogenitor cells and endosteal bone formation in mice lacking thrombospondin 2**. *J Bone Miner Res* 2000, **15**:851-862.

10. Beal MF: **Mitochondrial dysfunction in neurodegenerative diseases**. *Biochim Biophys Acta* 1998, **1366**:211-223.

Chapter IV

Future Directions

Summary of Results

Research conducted over the past decade has established the Wnt/β-catenin signaling pathway as a primary regulator of adipocyte differentiation [1-4]. Animal and human studies have extended prior *in vitro* observations and highlighted significant additional roles for Wnt/β-catenin signaling in disease processes such as obesity and type 2 diabetes [5-7]. Further complexity in the pathway arises from the regulated expression of endogenous inhibitors of Wnt signaling, including the family of secreted frizzled-related proteins (sFRPs). Numerous reports have shown that sFRPs inhibit Wnt signaling *in vitro* and *in vivo* by competitively binding Wnt ligands or frizzled receptors and blocking downstream activation of the pathway [8-11]. However, recent studies have confirmed additional roles for sFRPs that are independent of their classical Wnt-inhibitory function [12].

Here we report the finding that sFRP5 expression is dramatically induced during adipocyte differentiation of 3T3-L1 cells in culture (Figure 2.1a). Analysis of adipocytes and stromal vascular cells from adipose tissue yielded results consistent with those previously reported by Koza et al. [13], who showed that sFRP5 is expressed predominantly in the adipocyte fraction (Figure 2.1b). Koza

et al. also found that sFRP5 expression is correlated with increasing weight gain [13]. Here we extend those findings to show that sFRP5 expression is highly correlated with increasing adiposity and relative adipocyte size in multiple models of diet-induced and genetic obesity (Figure 2.2). Further evidence in support of an association between sFRP5 and adipocyte size comes from our studies using LXRβ -/- mice, the adipocytes from which do not undergo diet-induced hypertrophy. We found that while sFRP5 expression is increased 25 fold in high fat-fed wild type mice compared to low fat fed-controls, levels of sFRP5 mRNA are not different in LXRβ -/- mice under the same conditions (Figure 2.2d). Together, these results point to a strong correlation between sFRP5 expression and adipocyte expansion during obesity.

As sFRP5 expression in adipose tissue is elevated in every model of obesity analyzed, we sought to characterize the role of sFRP5 using genetically modified, loss-of-function mice. Here we show that sFRP5^{Q27stop} mice resist diet-induced obesity as evidenced by a decrease in total body weight and a reduction in fat mass, with no differences observed in the weight of other tissues (Figure 2.3, and data not shown). Investigation of circulating factors suggests that both fed insulin and leptin are decreased in sFRP5^{Q27stop} mice, possibly secondary to the decrease in fat mass observed by DEXA (Figure 2.3e).

A detailed examination of adipose tissue from wild type and sFRP5^{Q27stop} mice revealed that loss of sFRP5 limits the creation of large (> 8000 μm^2) adipocytes (Figure 2.4c). As sFRP5^{Q27stop} mice resist diet-induced weight gain, we questioned whether the observed effect on adipocyte size was a tissue

autonomous effect or simply a result of decreased adiposity in these animals. To address this question, we performed an adipose tissue transplant experiment wherein portions of gonadal white adipose tissue (G-WAT) from wild type and sFRP5^{Q27stop} donors were transplanted into *db/db* recipients to rapidly drive adipocyte hypertrophy of the donor tissue (Figure 2.4e). In agreement with our previous finding, analysis of donor G-WAT before and after transplantation showed that sFRP5^{Q27stop} adipose tissue contains proportionally fewer large adipocytes compared to controls (Figure 2.4f).

To identify the underlying cause limiting the creation of large adipocytes in sFRP5^{Q27stop} mice, we analyzed mRNA expression of factors known to play a role in vascular formation and recruitment of new vessels during obesity. However, our results indicate that vascular markers Ang-1, Ang-2, Tie-1, Tie-2, and ACTA2 are not altered in sFRP5^{Q27stop} G-WAT compared to controls (Figure 2.5a).

We also investigated the metabolic profile of sFRP5^{Q27stop} mice using a comprehensive lab animal monitoring system (CLAMS) to measure oxygen consumption, carbon dioxide production, respiratory quotient, and activity. The results of these studies suggest that in general, whole body metabolism of sFRP5^{Q27stop} mice is similar to that of wild type controls, with the unanticipated exception that carbon dioxide production appears to be decreased in sFRP5^{Q27stop} mice (Figure 2.6).

To further elucidate the role of sFRP5 in adipocyte biology, we utilized both immortalized and primary cell culture models of adipogenesis. Here we show that 3T3-L1 adipocytes overexpressing sFRP5 form larger and more

numerous adipocyte clusters than control cells, whereas sFRP5-depleted 3T3-L1 cells exhibit very little adipocyte clustering (Figure 2.7a). To extend this finding, we performed an adipocyte aggregation experiment in which 3T3-L1 adipocytes expressing either a scrambled control or two shRNA molecules against sFRP5 were detached from the culture dish and re-plated on various ECM substrates. Our data suggest that control adipocytes readily form large aggregates upon re-plating, while sFRP5-deficient adipocytes completely fail to form aggregates, and instead adhere to the substratum as mostly single cells (Figure 2.7b).

In light of the recent finding that integrins regulate clustering of 3T3-L1 adipocytes, we sought to determine whether the sFRP5 and integrin pathways interact utilizing a model of 3D collagen gel contraction, which has been shown to be dependent on integrin function. Interestingly, our results show that sFRP5-overexpressing preadipocytes contract collagen gels at an increased rate compared to controls, and that this effect is dependent on functional integrin $\beta 1$ (Figure 2.7c). Furthermore, we also show that phosphorylation states of focal adhesion kinase (FAK) and extracellular signal-regulated kinases 1/2 (ERK1/2), two downstream components of integrin signaling, are altered in sFRP5-deficient 3T3-L1 adipocytes and in primary ear mesenchymal stem cells (eMSCs) derived from sFRP5^{Q27stop} mice (Figure 2.7d).

Finally, we present data suggesting that loss of sFRP5 may lead to changes in cortical bone mass, local adipocyte metabolism, and temperature-dependent alterations in food intake (Figure 3.1, 3.2, and 3.3).

In summary, we have provided evidence that sFRP5 regulates adipocyte growth during obesity in a tissue autonomous manner, and that this effect may be mediated by integrin signaling. Though our results speak to a novel function for sFRP5 in adipocyte biology and obesity, many questions remain unanswered. In this chapter we outline some of these questions and discuss possible mechanisms by which sFRP5 may affect adipocyte function in light of our current understanding.

What Regulates sFRP5 Expression in Adipogenesis and Obesity?

Here we show that sFRP5 expression is increased substantially during adipocyte differentiation and in various models of obesity, displaying a strong positive correlation with percent body fat and relative adipocyte size (Figure 2.1, 2.2). However, the factors regulating sFRP5 expression under these circumstances remain unknown. While one published report indicates that the LIM-homeodomain transcription factor Lhx5 increases expression of sFRP5 in the forebrain [14], no studies have yet been published regarding regulation of sFRP5 in adipose tissue.

Perhaps more than any other cell type, adipocytes undergo dramatic changes in cell size under physiological conditions. Based on our previous results from the adipose tissue transplant described in chapter II, sFRP5 appears to be involved in controlling adipocyte hypertrophy during obesity (Figure 2.4f). However, this does not discount the possibility that sFRP5 expression may originally be upregulated by the initiation of hypertrophy in these cells. Support

for this hypothesis comes from our analysis of sFRP5 expression in high fat-fed LXRβ -/- mice where we observed no increase in sFRP5 expression in the absence of diet-induced adipocyte hypertrophy (Figure 2.2d). It is possible that as cell volume begins to increase under a growing lipid load, sFRP5 may be upregulated by increases in receptor signaling from the expanding cell membrane. Though speculative at this stage, recent evidence suggests that changes in cell volume may act as signals for basic cellular functions [15] and that cell volume changes may activate plasma membrane receptors including tyrosine kinase receptors, G-protein coupled receptors, and integrins, which are also known to participate in the regulation of cell size [16]. Thus, sFRP5 may be upregulated by increased activity of signaling pathways in expanding adipocytes, and in turn function to further influence adipocyte growth under conditions of obesity.

Another possibility involves an indirect mechanism for increasing sFRP5 expression in large adipocytes. It is well established that insulin sensitivity is inversely correlated with adipocyte size [17,18]. Thus, as adipocyte volume increases to facilitate lipid storage, sFRP5 upregulation may occur secondary to the development of insulin resistance in these cells. Future experiments to test this hypothesis should analyze sFRP5 expression in adipocytes from AMPKα2 -/- mice, or a similar model which exhibit an increase in adipocyte size without attendant insulin resistance [19].

Which Signaling Pathways Mediate sFRP5-Dependent Effects?

Classical models of sFRP function suggest that these factors bind to and sequester Wnt ligands in the extracellular space, blocking interaction with Frizzled receptors and preventing downstream activation of the pathway. To date, there have been no published reports of endogenous Wnt ligands expressed in mature adipocytes, which if true suggests that sFRP5 does not function by binding Wnts secreted by adipocytes. Recent reports, however, have provided evidence for additional mechanisms whereby sFRPs influence cellular processes. Studies proposing direct activation of Frizzled receptors by sFRPs independent of Wnt ligands are particularly interesting [20,21] and provide a premise for hypothesizing that sFRP5 may affect adipocyte function by directly signaling through frizzled receptors. Although Wnt/β-catenin signaling is suppressed during adipogenesis [4], the possibility exists that non-canonical or other signaling may be initiated through sFRP5/Frizzled interactions. To test this hypothesis, expression patterns of Frizzled receptors should be evaluated in adipocytes to rule out those that are not expressed. Frizzled receptors displaying appropriate expression patterns could then be evaluated for biochemical and genetic interaction with sFRP5 in cell culture and animal models.

sFRPs contain two main domains, a cysteine-rich domain (CRD) homologous to the CRD in Frizzled receptors, and a Netrin domain (NTR) homologous to a domain of the same name in Netrin molecules, which have well-established roles in axonal guidance [22]. Little has been published with regard to the function of the NTR domain in sFRPs, although there are intriguing parallels between our observations of sFRP5 function and those reported for

Netrin-1. For example, Netrin-1 affects axon attraction and outgrowth through activation of FAK [23-25] and we observed a decrease in FAK phosphorylation in two models of sFRP5-deficient adipocytes (Figure 2.7d). Additionally, activation of retinal neurons by Netrin-1 has been shown to stimulate protein synthesis and degradation through the ERK1/2 and ubiquitin pathways, respectively [26,27]. Similarly, we found that sFRP5 influences ERK1/2 phosphorylation in adipocytes (Figure 2.7d) and that several factors involved in the ubiquitination pathway are significantly altered in our microarray analysis of adipose tissue from sFRP5^{Q27stop} mice (Table 3.1). Furthermore, the fact that Netrin-1 interacts with its receptor via the netrin domain [28], a domain shared by sFRP5, leads to the speculation that sFRP5 may interact with and signal through netrin receptors in adipocytes. To test this hypothesis, functional studies involving deletion of the NTR domain in sFRP5 should be performed, in addition to assays examining a biochemical interaction between sFRP5 and Netrin receptors.

In addition to interaction with Frizzled or Netrin receptors, our finding that the integrin/ERK pathway is altered in cells lacking functional sFRP5 supports an additional model in which sFRP5 interaction with integrins at the cell surface influences adipocyte function through activation of integrin signaling. Previously, it was reported that sFRP2 can influence cell adhesion and apoptosis through interaction with fibronectin and integrin $\alpha5\beta1$ in MCF7 cells [29]. Furthermore, it has been shown that integrin $\alpha6$ is induced during adipocyte differentiation and regulates adipocyte clustering [30], two findings that parallel our observations with sFRP5 in 3T3-L1 cells (Figure 2.1a, 2.7a). Also, our data support a

functional interaction between sFRP5 and integrin β1 in the contraction of 3D collagen gels (Figure 2.7c). Taken together, our results suggest that sFRP5 may exert effects on adipocyte biology at least in part through interactions with the integrin cascade. While we show that activation states of ERK1/2 and FAK are altered in sFRP5-deficient adipocytes (Figure 2.7d), further evidence of a direct interaction with the integrin pathway is needed to confirm this hypothesis. Co-immunoprecipitation of candidate integrins, such as integrins α6 or β1, with sFRP5 should be performed to test whether these factors physically interact. In this regard, it is interesting to note that Netrin-1 has been shown to influence cell adhesion through direct interaction with integrin α6β4 via its NTR domain [31], the domain shared with sFRP5. Moreover, inhibiting the function of integrins in adipocytes with commercially available blocking antibodies would test whether sFRP5-mediated effects are dependent on integrin function in this context.

Thus, further attempts to elucidate the mechanism by which sFRP5 affects adipocyte function should investigate non-classical roles of sFRPs, including the interaction of sFRP5 with the cell surface receptors and pathways described above.

Which Cell Types are Targeted by sFRP5?

While our data suggest that sFRP5 acts in an autocrine/paracrine manner to influence adipocyte function, it is possible that sFRP5 may also signal to other cell types in the surrounding microenvironment. Under these circumstances,

rather than functioning as a signaling molecule, sFRP5 may act as an extracellular factor capable of performing diverse functions.

For example, in the context of obesity where neovascularization of adipose tissue is required to meet the energy needs of expanding adipocytes, an increased concentration of ECM-bound sFRP5 surrounding large adipocytes may serve as a guidance cue to recruit new microvessels to the cells in greatest need of nutrients. Likewise, as cells expand and approach maximum lipid-storing capacity, high levels of sFRP5 may act to recruit macrophages to those cells for breakdown and disposal. This hypothesis is supported by the finding that there are fewer crown-like structures (CLS) in adipose tissue from sFRP5^{Q27stop} mice compared to wild type controls (Figure 2.4d), though this observation may simply be secondary to differences in the obesity dependent inflammatory state of these animals. Both hypotheses presented above should be tested with migration assays utilizing sFRP5-producing cells as the source.

In addition to macrophages and vascular cells, adipose tissue contains resident adipocyte precursors, termed preadipocytes, which can be mobilized as needed to increase the number of lipid-storing adipocytes within the tissue. As Wnt signaling has been shown to act in an autocrine manner to maintain preadipocytes in an undifferentiated state [1], a model emerges in which sFRP5 is secreted at high concentrations from large adipocytes and feeds back to inhibit Wnt ligands secreted by preadipocytes, thus allowing these cells to differentiate and facilitate increased lipid accumulation during obesity (Figure 2.8). Although this hypothesis seems reasonable, our data indicate that overexpression of

sFRP5 in 3T3-L1 preadipocytes does not result in spontaneous adipogenesis (data not shown), suggesting that sFRP5 does not inhibit endogenous Wnts expressed by these cells. However, it is entirely possible that enforcing ectopic expression of sFRP5 in preadipocytes is not an accurate representation of paracrine signaling between adipocytes and preadipocytes in adipose tissue. Furthermore, preadipocytes may not contain the necessary processing machinery to correctly fold, package, or secrete an adipocyte protein such as sFRP5. Thus, until purified recombinant sFRP5 protein becomes available for use, we cannot conclude that sFRP5 does not function to block Wnt signaling in preadipocytes.

In summary, though our data support a novel, autocrine/paracrine role for sFRP5 in adipocyte biology, it is clear that further research will be needed to determine the effects of sFRP5 on all components of adipose tissue during obesity.

References

1. Ross SE, Hemati N, Longo KA, Bennett CN, Lucas PC, Erickson RL, MacDougald OA: **Inhibition of adipogenesis by Wnt signaling**. *Science* 2000, **289**:950-953.

2. Bennett CN, Ross SE, Longo KA, Bajnok L, Hemati N, Johnson KW, Harrison SD, MacDougald OA: **Regulation of Wnt signaling during adipogenesis**. *J Biol Chem* 2002, **277**:30998-31004.

3. Wright WS, Longo KA, Dolinsky VW, Gerin I, Kang S, Bennett CN, Chiang SH, Prestwich TC, Gress C, Burant CF, et al.: **Wnt10b inhibits obesity in ob/ob and agouti mice**. *Diabetes* 2007, **56**:295-303.

4. Moldes M, Zuo Y, Morrison RF, Silva D, Park BH, Liu J, Farmer SR: **Peroxisome-proliferator-activated receptor gamma suppresses Wnt/beta-catenin signalling during adipogenesis**. *Biochem J* 2003, **376**:607-613.

5. Longo KA, Wright WS, Kang S, Gerin I, Chiang SH, Lucas PC, Opp MR, MacDougald OA: **Wnt10b inhibits development of white and brown adipose tissues**. *J Biol Chem* 2004, **279**:35503-35509.

6. Guo YF, Xiong DH, Shen H, Zhao LJ, Xiao P, Guo Y, Wang W, Yang TL, Recker RR, Deng HW: **Polymorphisms of the low-density lipoprotein receptor-related protein 5 (LRP5) gene are associated with obesity phenotypes in a large family-based association study**. *J Med Genet* 2006, **43**:798-803.

7. Grant SF, Thorleifsson G, Reynisdottir I, Benediktsson R, Manolescu A, Sainz J, Helgason A, Stefansson H, Emilsson V, Helgadottir A, et al.: **Variant of transcription factor 7-like 2 (TCF7L2) gene confers risk of type 2 diabetes**. *Nat Genet* 2006, **38**:320-323.

8. Bafico A, Gazit A, Pramila T, Finch PW, Yaniv A, Aaronson SA: **Interaction of frizzled related protein (FRP) with Wnt ligands and the frizzled receptor suggests alternative mechanisms for FRP inhibition of Wnt signaling**. *J Biol Chem* 1999, **274**:16180-16187.

9. Uren A, Reichsman F, Anest V, Taylor WG, Muraiso K, Bottaro DP, Cumberledge S, Rubin JS: **Secreted frizzled-related protein-1 binds directly to Wingless and is a biphasic modulator of Wnt signaling**. *J Biol Chem* 2000, **275**:4374-4382.

10. Satoh W, Matsuyama M, Takemura H, Aizawa S, Shimono A: **Sfrp1, Sfrp2, and Sfrp5 regulate the Wnt/beta-catenin and the planar cell polarity pathways during early trunk formation in mouse**. *Genesis* 2008, **46**:92-103.

11. Bhat RA, Stauffer B, Komm BS, Bodine PV: **Structure-function analysis of secreted frizzled-related protein-1 for its Wnt antagonist function**. *J Cell Biochem* 2007, **102**:1519-1528.

12. Bovolenta P, Esteve P, Ruiz JM, Cisneros E, Lopez-Rios J: **Beyond Wnt inhibition: new functions of secreted Frizzled-related proteins in development and disease**. *J Cell Sci* 2008, **121**:737-746.

13. Koza RA, Nikonova L, Hogan J, Rim JS, Mendoza T, Faulk C, Skaf J, Kozak LP: **Changes in gene expression foreshadow diet-induced obesity in genetically identical mice**. *PLoS Genet* 2006, **2**:e81.

14. Peng G, Westerfield M: **Lhx5 promotes forebrain development and activates transcription of secreted Wnt antagonists**. *Development* 2006, **133**:3191-3200.

15. Vazquez-Juarez E, Ramos-Mandujano G, Hernandez-Benitez R, Pasantes-Morales H: **On the role of G-protein coupled receptors in cell volume regulation**. *Cell Physiol Biochem* 2008, **21**:1-14.

16. Franco R, Panayiotidis MI, de la Paz LD: **Autocrine signaling involved in cell volume regulation: the role of released transmitters and plasma membrane receptors**. *J Cell Physiol* 2008, **216**:14-28.

17. Salans LB, Knittle JL, Hirsch J: **The role of adipose cell size and adipose tissue insulin sensitivity in the carbohydrate intolerance of human obesity**. *J Clin Invest* 1968, **47**:153-165.

18. Salans LB, Dougherty JW: **The effect of insulin upon glucose metabolism by adipose cells of different size. Influence of cell lipid and protein content, age, and nutritional state**. *J Clin Invest* 1971, **50**:1399-1410.

19. Villena JA, Viollet B, Andreelli F, Kahn A, Vaulont S, Sul HS: **Induced adiposity and adipocyte hypertrophy in mice lacking the AMP-activated protein kinase-alpha2 subunit**. *Diabetes* 2004, **53**:2242-2249.

20. Rodriguez J, Esteve P, Weinl C, Ruiz JM, Fermin Y, Trousse F, Dwivedy A, Holt C, Bovolenta P: **SFRP1 regulates the growth of retinal ganglion cell axons through the Fz2 receptor**. *Nat Neurosci* 2005, **8**:1301-1309.

21. Dufourcq P, Leroux L, Ezan J, Descamps B, Lamaziere JM, Costet P, Basoni C, Moreau C, Deutsch U, Couffinhal T, et al.: **Regulation of endothelial cell cytoskeletal reorganization by a secreted frizzled-related protein-1 and frizzled 4- and frizzled 7-dependent pathway: role in neovessel formation**. *Am J Pathol* 2008, **172**:37-49.

22. Jones SE, Jomary C: **Secreted Frizzled-related proteins: searching for relationships and patterns**. *Bioessays* 2002, **24**:811-820.

23. Li W, Lee J, Vikis HG, Lee SH, Liu G, Aurandt J, Shen TL, Fearon ER, Guan JL, Han M, et al.: **Activation of FAK and Src are receptor-proximal events required for netrin signaling**. *Nat Neurosci* 2004, **7**:1213-1221.

24. Liu G, Beggs H, Jurgensen C, Park HT, Tang H, Gorski J, Jones KR, Reichardt LF, Wu J, Rao Y: **Netrin requires focal adhesion kinase and Src family kinases for axon outgrowth and attraction**. *Nat Neurosci* 2004, **7**:1222-1232.

25. Ren XR, Ming GL, Xie Y, Hong Y, Sun DM, Zhao ZQ, Feng Z, Wang Q, Shim S, Chen ZF, et al.: **Focal adhesion kinase in netrin-1 signaling**. *Nat Neurosci* 2004, **7**:1204-1212.

26. Campbell DS, Holt CE: **Chemotropic responses of retinal growth cones mediated by rapid local protein synthesis and degradation**. *Neuron* 2001, **32**:1013-1026.

27. Campbell DS, Holt CE: **Apoptotic pathway and MAPKs differentially regulate chemotropic responses of retinal growth cones**. *Neuron* 2003, **37**:939-952.

28. Cirulli V, Yebra M: **Netrins: beyond the brain**. *Nat Rev Mol Cell Biol* 2007, **8**:296-306.

29. Lee JL, Lin CT, Chueh LL, Chang CJ: **Autocrine/paracrine secreted Frizzled-related protein 2 induces cellular resistance to apoptosis: a possible mechanism of mammary tumorigenesis**. *J Biol Chem* 2004, **279**:14602-14609.

30. Liu J, DeYoung SM, Zhang M, Zhang M, Cheng A, Saltiel AR: **Changes in integrin expression during adipocyte differentiation**. *Cell Metab* 2005, **2**:165-177.

31. Yebra M, Montgomery AM, Diaferia GR, Kaido T, Silletti S, Perez B, Just ML, Hildbrand S, Hurford R, Florkiewicz E, et al.: **Recognition of the neural chemoattractant Netrin-1 by integrins alpha6beta4 and alpha3beta1**

regulates epithelial cell adhesion and migration. *Dev Cell* 2003, **5**:695-707.